PROPERTIES OF THIN FILM $Li_xLa_yTiO_3$ ELECTROLYTE FOR ALL-SOLID STATE Li-ON BATTERIES

Sena GÜLEN

İzmir Institute of Technology

March, 2016

PROPERETIES OF THIN FILM $Li_xLa_yTiO_3$ ELECTROLYTE FOR ALL-SOLID STATE Li-ION BATTERIES

A Thesis Submitted
To the grade School of Engineering and Sciences of
Izmir Institute of Technology
In Partial Fulfillment of Requirement for Degree of

MASTER OF SCIENCE
In Physics

by
Sena GÜLEN

March 2016
İZMİR

We approve the thesis of Sena GÜLEN

Examine Committee Members:

Assoc. Prof. Dr. Gülnur AYGÜN ÖZYÜZER
Department of Physics, Izmir Institute of Technology

Asst. Prof. Dr. Mehtap ÖZDEMİR KÖKLÜ
Department of Electric and Electronical Engineering, Gediz University

Asst. Prof. Dr. Enver TARHAN
Department of Physics, Izmir Institute of Technology

10 March 2016

Assoc. Prof. Dr. Gülnur AYGÜN ÖZYÜZER
Supervisor, Department of Physics
Izmir Institute of Technology

Prof. Dr. Tuğrul SENGER
Head of the Department of Physics

Prof. Dr. Bilge KARAÇALI
Dean of the Graduate School of
Engineering and Sciences

ACKNOWLEDGEMENTS

First of all I would like to thank my supervisor Assoc. Prof. Dr. Gülnur AYGÜN for her excellent guidance, caring, patience, and providing me with an excellent atmosphere for doing researches throughout the projects.

Many thanks must go to my co-advisor Prof. Dr. Lütfi ÖZYÜZER for his advice, which is beyond price.

The thanks should go to the project director Asst. Prof. Dr. Mehtap KÖKLÜ of Gediz University who helped me during my thesis.

I also extend my thanks to Yasemin Demirhan, Hakan Alaboz, Halil Arslan from İzmir Institute of Technology.

I would also like to acknowledge that this research is partially supported by TUBITAK (Scientific and Technical Research Council of Turkey) project number 114M044.

At last but not least, there is no correct word to explain my lovely mother and father contribution to my education and explain their love and express my thanks for their helps. Additionally I am thankful to my lovely sister Hazal Gülen and brother Furkan Gülen, who always encouraged me for the master studies.

ABSTRACT

PROPERTIES OF THIN FILM $Li_xLa_yTiO_3$ ELECTROLYTE FOR ALL-SOLID STATE Li-ION BATTERIES

One of the requirements of daily life, the most preferred rechargeable batteries are Li-ion batteries because of high energy, long life cycle and eco-friendly properties. Having high energy density, no memory effect and slow energy losses, these batteries have applications in portable electronic devices, power source for space vehicles, electric cars etc. Furthermore, there is a strong interest in all solid-state rechargeable lithium-ion battery research, because these batteries will replace the conventional liquid electrolyte Li-ion batteries due to use of non-combustible inorganic solid electrolyte, which has high safety and reliability.

While the bulk ionic conductivity of $La_{0.5}Li_{0.5}TiO_3$ (LLTO) produced by solid-state reaction is 10^{-3} S/cm, the total ionic conductivity of LLTO is 10^{-5} S/cm. Another way to increase ionic property is to dope the solid electrolyte with transition metals. The substitution of transition metal leads to decrease of the lattice parameter because of reduced average ionic radius. This causes increase of Li-ion content and also ionic conductivity.

In this study, initially pure and Al doped targets were fabricated by using solid-state reaction after that the available targets are placed to the sputtering gun. When the all optimizations of the system were completed, pure and Al doped LLTO thin films were deposited by RF (radio frequency) magnetron sputtering technique on ITO coated soda lime glass substrates. While the thin film was been deposited, the substrate was heated at approximately 220 ^oC.

For ionic conductivity measurement of the Al doped LLTO electrolyte, small circular Al contact regions were created on Al doped LLTO thin films by thermal evaporation system. Afterword the impedance spectra of the sandwich structure in a frequency range of 1 Hz - 200 MHz was recorded by using probe station.

Thickness, the crystal structure, optical transmission, chemical compositions, surfaces and porosity of the thin films are investigated by surface profilometer, XRD, UV-Visible Spectroscopy, XPS, and Raman Spectroscopy respectively.

ÖZET

TAMAMEN KATI HAL Li-İYON BATARYALARI İÇİN İNCE FİLM $Li_xLa_yTiO_3$ ELEKTROLİTİNİN ÖZELLİKLERİ

Gündelik hayatın gereksinimlerinden biri olan şarj edilebilir bataryaların içinde ağırlıklarına ve büyüklüklerine oranla verebildikleri yüksek enerji, uzun yaşam döngüleri ve çevre dostu özelliklerinden dolayı Li-iyon pilleri çokça tercih edilmektedir. Tamamen katı hal, doldurulabilir lityum iyon piller uygulama açısından yüksek potansiyele sahiptir. Çünkü geleneksel sıvı elektrolitli lityum pillerin yerini alacak olan bu pillerin yanmayan inorganik katı elektrolit kullanılması dolayısıyla güvenilirliği yüksektir. Taşınabilir elektronik cihazlardan uzay araçları için güç kaynağına, elektrikli arabalara kadar yaygın kullanım alanına sahip olabilecek bu pillerde enerji yoğunluğu yüksektir ve hafıza etkisi yoktur.

Katı hal reaksiyonu ile üretilen $La_{0.5}Li_{0.5}TiO_3$ (LLTO)'nun yığın iyonik iletkenliği 10^{-3} S/cm gibi yüksek bir değere sahip olmasına rağmen çoklu kristal yapıdaki tanecikler arasındaki zayıf bağlar sebebi ile toplam iyonik iletkenlik 10^{-5} S/cm olarak bulunmaktadır. İyonik iletkenliği arttırmanın bir yolu katı elektrolit katmanını geçiş metalleri ile katkılamaktır. Geçiş metali olan alüminyum ile katkılanan LLTO katı elektrolitlerin kafes parametresi ortalama iyonik yarıçapın azalması nedeni ile küçülür. Böylece Li-iyon içeriği ve dolayısıyla iyonik iletkenlik seviyesi artacaktır.

Bu çalışmada alüminyum katkılı $La_{0.5}Li_{0.5}TiO_3$ (LLTO) katı elektrolit yüksek vakumda RF (radyo frekans) mıknatıssal saçtırma yöntemi ile ITO kaplanmış mikroskop camı üzerine alttaş ısıtılarak büyütülmüştür. Kalınlık, optiksel geçirgenlik ve yapısal analizler, yüzey ölçer, XRD, XPS, Raman Spektroskopisi gibi cihazlar kullanılarak yapılmıştır.

Al-katkılı ve saf LLTO ince filmlerin iyonik iletkenliği 1 Hz – 200 MHz frekans aralığında empedans analizörü ile prob istasyonunda ölçülmüştür. Bu ölçüm için saf ve Al katkılanmış LLTO ince filmler üzerine termal buharlaştırma yöntemi ile küçük dairesel alüminyum kontak alanları oluşturularak iyonik iletkenlik ölçümleri tamamlanmıştır.

Dedicated to

my lovely parents

TABLE OF CONTENTS

LIST OF FIGURES

Figures **Page**

LIST OF TABLES

Tables **Page**

CHAPTER 1

INTRODUCTION

1.1. Li-Ion Battery

In last century rapidly developing technology requires more energy sources for various type of electronic devices. The dramatic increase of the energy demands on the global world shows that ascendant energy storage regulation must be generated urgently. Not only wide range of energy reserve is enough for this shortage, but also emission of the carbon dioxide must be minimal. It also should be against of the rising prices and the alternative should be low cost as well. In last decay it has been seen that, reliance on petrol reserves is decreasing crucially. From this perspective the renewable energy is the most promising way that has wide alternative choices such as wind, solar cells to intercept of global warming and provide high efficiency (Shukla et al, 2008).

Recent years, lots of researchers are searching on sustainable energy supplies, which have either high power density or high reliability. The goal of these studies is that Li-based battery systems can be applicable to so many types of electronic devices, systems such as mobile phones, laptops, power supply systems, medical appliances, memory back-up, navigation aids, space craft and electric and hybrid vehicles (Linden, 1995).

While they provide high specific energy and energy density in less weight (gravimetric) or volume (volumetric), also they have low charge-discharge capability. In additionally there is no memory effect and Li-ion batteries present a low self-discharge rate and rapid charge capability (Simpson, 2011). Moreover energy production and storage processes are totally environment friendly because there is no toxic gasses effect on the ecology (Nong et al, 2015). However safety is the one of the fundamental problem for rechargeable li-ion batteries so to get rid of this disruption, stable batteries are needed at room temperature or high temperatures. Furthermore high air reactivity of lithium-metal brings a serious drawback for integration case (Zhangfeng Zheng & Wang, 2012).

1.2. All Solid-State Li-Ion Battery

All solid-state Li-ion batteries are mostly preferred in recent time. The main reason of this preference underlies determine, fixed and compact structure of the molecules such as glassy or polymer materials. The structural properties of the molecules can be summed up in one word as ‘’rigidity’’. Rigid structures have strong bonds at any given temperature so these molecules reach a good thermally stability. It is the fundamental structural quality but not all. At the same time rigid structures provide mechanical stability of shear resistance as well. Mechanical stability does not mean indestructible structure they have. Conversely many cracks can be occurred in solid crystals easily. Solid materials have advantages in order to get an intended shape and fabricate in smaller, thinner, or larger thicker sizes of desired samples (Kharton, 2009).

The other aspect of advantages of solid-state Li-ion battery is good ionic conductivity (Inaguma & Nakashima, 2013). Thanks to solids, which have kinematic reactions and thermal stability due to strong chemical bounds. This quality of solids, provide transport selectivity between anode and cathode layers. In this case it is the distinctive attribution of the electrolyte layer in the battery. Through transport selectivity, it is possible to get rid of polarization operation.

At last but not least all solid state Li-ion batteries are not only have thermal stability, good ionic conductivity, high energy and power density, but also there is no leakage and problem like as Li-ion batteries which have liquid electrolytes (Z. Zheng, Fang, Yang, Liu, & Wang, 2014). In additionally safety is another key quality for rechargeable Li-ion batteries. So the solid-state electrochemistry makes the Li-ion batteries are the major interested in subject all around the world.

Solid-state batteries can be a composition of polymers or inorganic materials. Electrolyte layer presents the most important role in all solid-state Li-ion batteries. In general, polymers include organic solvent so all the risks resemble the liquid ones. In additionally for high temperature, polymer electrolytes are inconvenient owing to disintegration of the atomic structure. For this reason polymers are not widely used as solid electrolyte material (Minami et al., 2006). The highest ionic conductivity, good thermal and electrochemical stability for solid electrolytes have the major interest. In comparison inorganic all solid-state batteries have large utility areas than liquid or polymer. For that reason, solid-state batteries are the most preferred Li-ion battery type in recent years.

There are two kinds of inorganic all-solid state batteries as crystalline electrolytes (LISICON, garnet type, perovskite-type and NISCON), and secondly glass based electrolytes (glassy, glassy ceramics) (Cao, Li, Wang, Zhao, & Han, 2014). Types of inorganic solid electrolytes will be discussed with more detail in fallowing chapters.

1.3. All Solid State Thin Film Li-Ion Batteries

Basically all solid state Li-ion battery composition consists of three main layers as solid electrolyte, negative and positive electrodes. There are two ways to compose this battery: bulk type or thin film (Inaguma & Nakashima, 2013).

New generation applications focus on minimized size and power requirement of application in consumer and medical electronics (Dudney & Neudecker, 1999). Miniature electronic devices are the heart of the so many types of innovations. For this reason improvement on rechargeable battery systems, which are applicable for many types of electronic devices, has a large scale of study area. In this case all solid-state batteries have the major interest due to compact, portable, safety, maximized energy density, thermal stability, high ionic conductivity. So that solid electrolyte of rechargeable Li-ion batteries has replaced of liquid or organic one. Because of the fact that, a new question has grown out about the type of the solid electrolyte (Z. Zheng et al., 2014).

Many aspects maintain the bulk electrolyte has higher ionic conductivity at room temperature because of the bulk crystal structure and less grain boundary. Composition of the bulk type solid rechargeable battery is created by active material for electrode, bulk electrolyte and conductive additive powders (0.3 mm) (Kharton, 2009). To evolve of the cell performance not only high ionic conductive solid material shows vital importance but also the smallest distance between electrode and the electrolyte plays a serious role (Minami et al., 2006).

Many study focus on all solid-state Li-ion batteries constructed by completely thin film layers (<5 μm) (Dudney & Neudecker, 1999). Parts of the battery as cathode, anode electrolyte and current collector are fabricated by one of the thin film deposition technique such as RF (radio frequency) magnetron sputtering (Xiong, Tao, Zhao, Cheng, & Zhao, 2011) (Bates, Dudney, Neudecker, Ueda, & Evans, 2000), pulsed laser deposition (PLD)(Aguesse et al., 2015) and electron-beam evaporation (Li, Zhang, & Fu, 2006).

Multi layered structure of thin film battery either has many opportunities for deposition layer by layer or many options to choose construct materials for the components of entire battery. Thus the trend of the properties can be matched separately with each other and several sorts of combinations can be derived for nano-technology devices.

Thin film technology is the greatest originality, which incorporates the battery world with microelectronic devices as differently from the conventional battery systems. All solid-state inorganic thin film batteries are considerably promising that maximum energy density in minimum volume, maximum thermal and electrochemical stability and the highest ionic conductivity at high and high temperatures with ultra-safety and environmental friendly qualities. So recently, it has the major interest in literature and consumer applications in wide spread area (Nong, Xu, Yu, Zhu, & Yu, 2015).

In light of foregoing, inorganic, solid thin film type of electrolyte layer is studied for an entire all solid-state rechargeable Li-ion battery system, which is applicable for hybrid-electric vehicle or pure electric vehicle. Thin film LLTO ($Li_{0.5}La_{0.5}Ti_{1-x}Al_xO_3$) electrolyte has the best electrochemical properties and maximum energy density in minimum volume to get the highest ionic conductivity (Xiong et al., 2011). The target of this study can be summarized as fabrication of solid inorganic LLTO electrolyte layer, which has the maximum ionic conductivity value by using thin film technology.

1.4. Classification of Cells and Batteries

Electrochemical cells and batteries can be classified as primary batteries (non-rechargeable) and secondary batteries (rechargeable). This classification is based on electrically rechargeable ability. The identification of the battery types is not only possible due to being recharge but also it is possible for composition of structure or designs. Each type has advantages or disadvantages separately. However in recent years rechargeable cells or batteries for consumer applications or medical applications have attracted much attention (Linden, 1995).

1.4.1. Primary Li-Ion Batteries

Primary batteries are very sufficient for variety of low cost consumer applications such as toys, portable electrical or electronic portable devices, and memory backups. The

main advantage of primary battery is lightweight source for packaged power, lower initial cost and longer operation charge. Furthermore maximum energy density primary batteries are widely used in military executions for instance signaling devices or standby power equipment (Linden, 1995).

However higher life cycle cost ($/kWh), disability of electrochemically recharge, limit to usage for specific applications. The life cycle energy efficiency is not so high and they can be used just once.

Some of the examples are: carbon/zinc is can be used for radios, electronic toys; Mg/MnO_2 is applicable for military or aircraft receiver; $Zn/Alkaline/MnO_2$ is suitable for calculators, radios, televisions; Zn/HgO has usage on hearing aids, photography, military sensors; Li/MnO_2 is widely used in medical devices, memory circuits and Zn/Ag_2O is preferred for watches, photography. In contrast, primary batteries are not convenient for such as high cost hybrid automobiles, cell phones, or laptops (Cambridge-University, 2016).

1.4.2. Secondary Batteries

Secondary batteries are rechargeable so they play a leading role in daily life. Because, rechargeable batteries which are the key devices for such as laptops, mobile phones. They have either high power density and discharge rate or good low temperature performance. While charge retention and energy densities are not high as the primary batteries, recharging cycle can restore the capacity of secondary batteries (Linden, 1995).

Mainly secondary batteries can be divided into two kinds. The first one is applicable for energy storage devices, which are connected to energy source and getting charge after than transfer the stored energy as needed. These batteries are suitable for hybrid electric vehicles or aircraft systems (Linden, 1995).

The other type of secondary batteries runs like the primary batteries. The discharging process works on as the same but they can be recharge after use so the recharge process depends on demand for replaced. These types of batteries are convenient for electric vehicles, power tools, and consumer applications.

Some of the main examples of secondary batteries: Lead-acid is applicable for uninterruptible power supply (UPS), emergency lightening; Nickel-Cadmium is used for medical applications; Nickel-metal-hydrate is suitable for medical instrument and hybrid

electronic vehicles; Lithium-ion is the most popular one which can be apply for power tools, medical instruments, as well as hybrid and electric vehicles automotive and energy storage systems (Battery-University, 2016).

1.4.3. Reserve Batteries

The reserve batteries do not provide power up to activated. These kinds of batteries are generally appropriate for variety of military applications because of the high power quality and long-term storage period. Although the usual primary batteries are at rest to get rid of loss while storing, likewise while running operation, the system is active to get high performance, the reserve systems either active or inactive position can be perform separately. While it has high power, it has not high-energy density as much as primary batteries. Basically, primary batteries can be used in a short time after activation period so they are applicable for missiles or torpedoes (Ritchie & Bagshaw, 1996).

There are four main types of reserve batteries as water activated, electrolyte-activated, gas activated, heat activated (thermal) batteries (Linden, 1995).

1.4.4. Fuel Cells

Fuel cell working principle is similar because both of them convert the chemical energy to electrical energy. But fuel cells use a fuel and oxidant for this transformation externally so the main difference is energy production source between fuel cells and batteries.

While the fuel cells generate energy, electrodes use the active material and the electrodes are generally constructed by inert materials to avoid run out of them. As an anode active material mostly gas or liquid fuels are preferred.

There are two types of fuel cells as direct and indirect systems. In direct systems the anode active material like hydrogen, methanol or hydrazine directly behaves as a reactant. But, for indirect systems natural gas or fossil fuel is initially converted to a hydrogen rich gas, after this process anode active material can play an active role for conversion of the energy (Linden, 1995).

1.5. All-Solid-State Lithium Secondary Batteries

All-solid-state lithium secondary batteries have the major interest in last decays. The innovations on technology bring new requirements for wide variety of applications. Furthermore to give a convincing answer, first of all the energy source and storage system must be introduced which may replace by the conventional ones. Inorganic solid electrolytes are the most promising for reliable lithium ion batteries. To create all-solid-state battery as powder or thin film formation of solid electrolyte must be fabricated initially to meet any demand. Moreover electrodes and conductive additives can be designed for high electrochemical cell performance of multi-layered structure of all solid-state thin film batteries (Minami et al., 2006).

1.5.1 Components of Battery

Last breakthroughs in technology bring new design alternatives and materials for batteries. Basically batteries are the systems that convert the electrical energy through the mechanical energy by redox reactions. In order to get high efficiency from the electrochemical reactions new generation materials blaze a trail. Thus, so many variations of orientations and matching options of the electrochemical compounds help to derivate new mechanisms.

For high ionic conductivity of Li-ion batteries the key word is electrolyte layer, which should provide selective transition of Li-ions between positive and negative electrodes during charging or discharging periods. In order to demonstrate the different types or compositions of anode (negative electrode), cathode (positive electrode) and electrolyte layer, which are the components of the all solid-state Li-ion battery will be checked over in details by next subheads separately.

1.5.1.1. Anodes

Anodes are the negative electrolytes, which are generally fabricated by variations of carbon, especially graphite widely used (IJESD, 2000). Because carbon materials have high specific capacity (370 $mAhg^{-1}$), good stability, low cost and easy for fabrication. But in electrochemical perspective, transition of Li-ions can not move reversibly into the

carbon layer through the inorganic solid electrolytes ($60Li_2S.40SiS_2$ (mol%)). For this reason it is not appreciate for negative electrode material of all solid-state battery.

One of the most useful negative electrode materials with inorganic solid electrolytes is indium. However this material can not preferred so much because of the high cost (Minami et al., 2006).

The other anode material choice for all solid-state battery is lithium silicide. It has high specific capacity and negative potential which is pending to metallic lithium (approximately 0.3 V) (Minami et al., 2006). In addition it does not include toxic elements so it is eco-friendly material.

As a result meta-stable ($Li_{4.4}Si$) alloy is the most promising attractive anode material for charge or discharge cycle for all solid-state batteries (Minami et al., 2006). Alternatively zinc is also convenient anode material for Li-ion batteries (Linden, 1995).

For the most beneficial anode cathode combination should be not only practically as lightweight, high capacity but also has good reactivity between each other components.

1.5.1.2. Cathodes

Cathodes are the positive electrodes that generally produce by metal oxides such as $LiCoO_2$, $LiFePO_4$, $LiNiO_2$, $LiMn_2O_4$, WO_3, V_2O_5, TiS_2. Especially cobalt is a high cost material so it is not used actively while it has the highest theoretical energy storage capacity. The mostly used cathode material is $LiFePO_4$, has the highest thermal stability and fast charging or discharging rate than the other whereas $LiNiO_2$ has practically the highest energy storage capacity (Chagnes, 2015).

Additionally $LiMn_2O_4$ with oxygen ions generally has spinal atomic cage in face-centered cubic structure and the lithium with manganese ions occupy tetrahedral and octahedral structure. Aluminum doped manganite is an alternative cathode material has either not higher cost than the other or better performance (IJESD, 2000).

As a result in comparing cobalt and nickel materials as positive electrode, nickel is not as desirable as cobalt. The mean reason of this preference can be summarized as stability of the material. Because while cobalt makes Li-ions 50% move reversibly, nickel makes 70%. In fact cobalt transform less stabile form at the end of the charging.

On the other hand for high energy density lithium batteries one of the attractive cathode material is sulfur because of the high specific capacity (theoretically 1067 $mAhg^{-}$

[1]). Combination with inorganic solid electrolyte can not transported lithium ions through the polysulfide while discharging. For this reason elemental sulfur is more attractive cathode material for all solid-state Li-ion battery charging or discharging periods.

1.5.1.3. Electrolyte

Electrolyte is the most important layer of the battery that transfers of lithium ions and provides good ionic conductivity between positive and negative electrode. Furthermore to prevent discharge, blocks the electron transfer and provide selective and high ionic conductivity.

Many types of electrolytes can applied for Li-ion batteries. There are three main classification for electrolyte as liquid, polymer and solid state (Daniel, 2008). Generally preferred liquid electrolytes are $LiBC_4O_8$ (LiBOB), $LiPF_6$ and $Li[PF_3(C_2F_5)_3]$ in organic alkyl carbonate solvent. But these electrolytes are imperilment because of flammability or explosion risks. The reason of this danger is week thermal stability at room temperature (Sloop, Pugh, Wang, Kerr, & Kinoshita, 2001).

In contrast, thin film electrolyte can be possible by using the polymer based (Monroe & Newman, 2005). The difference between liquid or solid electrolyte is the usage of a solvent such as polyethylene oxide (PEO), which includes $LiPF_6$. The advantage of polymer electrolyte is not only make possible thin film applications, but also no limitation for forming, high charging or discharging cycle and high power density. There are four materials generally preferred for polymer electrolyte as; polyacrylonitrile (PAN), polyvinylidene fluoride (PVdf), polymethyl methacrylate (PMMA) and polyethylene oxide (PEO).

In last decays PVDF polymer electrolyte is preferred for Li-ion batteries because of the high concentration of carriers (Esterly, 2002).

Solid-state electrolytes have the highest potential due to safety and reliability then the conventional liquid or polymer electrolyte. The leakage and flammability are the most serious problems for the electrolyte. To get rid of these kinds of problems of the conventional batteries, inorganic solid electrolytes, which is a layer of new generation all-solid state batteries, are preferred for wide application areas in the world (Chagnes, 2015). Solid electrolytes for all solid-state batteries can be divided by two main categories as crystalline electrolyte and glass-based electrolyte. The most important ones are

LISICON, thio-LISCON $Li_{10}SnP_2S_{12}$, garnet $Li_7La_3Zr_2O_{12}$, perovskite $Li_xLa_yTiO_3$, NASICON $Li_{1.3}Al_{0.3}Ti_{1.7}(PO_4)_3$, glass-ceramic $xLi_2S.(1\text{-}x)P_2S_5$.

LISICON-type solid electrolyte has not high ionic conductivity as thio-LISICON at room temperature (Cao et al., 2014). For high ionic conductivity garnet-type $Li_7La_3Zr_2O_{12}$ (LLZO) has good stability for all solid-state Li-ion batteries, which has starting discharge capacity 93 $mAhg^{-}1$ at 50 ^oC when composed with $Cu_{0.1}V_2O_5$ and Li electrodes.

NISICON-type electrolytes have good stability and ionic conductivity but if they compared by the perovskite lithium-lanthanum-titanates, they would not have the highest stability and ionic conductivity (Cao et al., 2014).

Glassy electrolytes have major interest because of, none of grain boundary resistance. Also they can be fabricated as thin film to apply numerous electronic devices. They can be investigated in two oxides and sulfides. Although sulfide glasses have high ionic conductivity at room temperature, the oxide glassy electrolytes have lower ionic conductivity. For all solid-state batteries glass electrolytes can be preferred in terms of easy synthesis opportunity (Cao et al., 2014).

In familiar perovskite-type electrolyte is the lithium-lanthanum-titanates (LLTO) with perovskite structure (ABO_3). It has the most favorable solid electrolyte because the reduction of Ti^{+4} to Ti^{+3} provides decreasing of electronic conductivity. (Chen, Liang, Zhang, Wu, & Li, 2012). The most important property is that diminishing of the grain boundaries. Thus ionic conductivity gets the highest value.

In this thesis for all solid-state batteries, $Li_{0.5}La_{0.5}Ti_{1-x}Al_xO_3$ solid-state inorganic thin film electrolyte is studied with characterization as can be seen in details in next chapters. To increase the ionic conductivity value of the electrolyte layer aluminum doping is done. Thus the atomic radius was increased and grain boundaries are decreased so higher ionic conductivity is observed.

The other originality of this study is while depositing the thin film, the substrate is heated at the same time. After deposition the thin films annealed at different temperatures to observe crystallinity

1.6. From Cells to Packs Formations for Li-Ion Batteries

1.6.1. Cells, Modules and Packs for Batteries

The basic electrochemical unit of a battery is called cell, which converts the electrical energy to chemical energy. A battery has many cells and each cell has electrolyte, electrode and separator and connected as series or parallel circuit for desired voltage (Linden, 1995). Efficiency of a cell is generally different from the multi-cell battery system. Because each cell create a resistivity separately for this reason representation of battery performance mostly shows the total performance of the cells, which are constructed in a battery.

A number of cells become together and constitute a module, which has over charge or discharge control circuit to protect the battery. Generally combination of 6 or 12 cells are using for electric vehicles.

Furthermore the modules are brought together and created battery packs. As an example Li-ion battery for the first electric vehicle (Nissan Altra) includes 12 x eight-cell modules and while the total weight of the battery pack is 364 kg, the total weight of the cells is 317 kg. The lost 47 kg is for circuitry for module packing. As volumetric calculation, the dimensions are 100 cm x 200 cm x 18 cm approximately (IJESD, 2000).

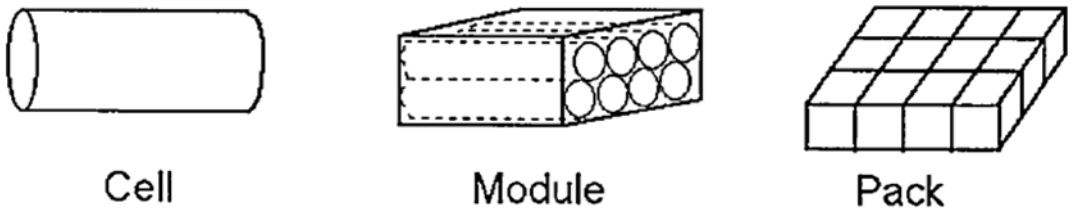

Figure 1. 1. Cell to pack formation
(Source: Linden, 1995).

1.6.2. Cell Geometry

In common, the cylindrical cell is the most favorable for primary and secondary batteries because of the high mechanical stability performance, easy to produce and high internal pressures to avoid deformation. Lithium and nickel based cylindrical cells have a positive thermal coefficient tool. Due to current, the polymer, which is a conductive

material in normal condition, gets warm and transformed to resistive form. In this way the current is paused so short circuit conservation is occurs. When the short circuit is ceased and the thermal coefficient becomes cold. At the end is transformed to conductive state.

If a danger occurs, the pressure valve, which is connected to electrical fuse by Li-ion cell, opens immediately. These types of cells are applicable for portable applications such as laptops, power equipment and medical instruments.

Another geometry for cells is coin-shaped (button cell) which are aimed higher cell voltages. These cells are suitable for watches, cordless telephones, security wands and variety of medical devices such as medical implants, hearing aids, which have primary (non-rechargeable) batteries.

For flexible shaped batteries the prismatic cell is convenient. But it has less attractive for thermal operations and it is high cost design. Additionally, it has not long cycle life as the cylindrical cell.

The highest battery pack efficiency is provided by pouch cell. Non-usage of metal is decreasing the weight of the cell. But as mechanically it needs to expand in battery. Generally, Li-polymer batteries are created by pouch cells and they are used for portable applications.

1.7. Operation of a Cell

If there is an external load, which is connected to a battery cell, the ions flow from the anode through the cathode. For transfer of the ions the electrolyte layer is passed through to reach cathode layer. When the ions are transferred to cathode, reduction reaction is occurred. This period called discharging.

Oppositely, while the cell is charging the ions move from the cathode through the anode by passing through the electrolyte layer. The battery stores the energy during this period. When there is no ion for transfer, the battery reaches the full energy level.

For Li-ion batteries, electrons can not transferred passing through the electrolyte in both cases, only ions are allowed to transfer.

1.8. Future of Li-ion Batteries

In variety of electrolyte, anode and cathode combination the key is that can be selected the most convenient electrolyte material. In recent years the solid electrolyte takes the liquid and polymer electrolyte places because of it has high ionic conductivity quality and in minimum value and weight with maximum energy density additionally inflammable and ecological friendly attribution with low cost production. However not at least, Li-air battery is the new technological innovation for many types of applications (Nong et al., 2015).

CHAPTER 2

ALL-SOLID-STATE THIN FILM Li-ION BATTERIES

All solid-state rechargeable lithium ion batteries have high potential in order to application. This type of batteries will replace the conventional liquid electrolyte lithium ion batteries because of their combustible inorganic solid electrolyte component, which has safety features. Lithium batteries are the most demanded type of eco-friendly rechargeable batteries in daily life with their features of high-energy capacity despite of their weight and size. The batteries are using in various areas like portable electronic devices, power supply of spacecraft, and electric vehicle. Lithium ion batteries have high density of energy, no memory effect and low loss of energy when it is out of use. Lithium ion batteries have lower weight when it is compared with the equivalents, which are

prepared by various types of chemicals. The reason of this is top level 160 Wh/kg filling density. World trade volume for lithium ion batteries was 5 billion dolars in 2005 and it is expected to reach over 2 billion euros in 2022. With higher production of eco-friendly hybrid and completely electrically powered vehicles, the demand for rechargeable batteries will increase.

A conventional lithium battery contains a cathode, anode and electrolyte. The anode is usually composed of materials containing carbon such as graphite or carbon fibers. Because carbon can make easily intercalation. Oxide, which usually consists of cathode electron donor like $LiMO_2$ (M=Co, Ni, Mn). Electrolyte separates the anode from the cathode. Any electrolyte of battery environment should provide ionic conduction between positive and negative electrodes in cell and should be selective and have high conductivity for ions, which is in electronic reaction. However it should not transmit electrons to prevent the discharge. Solid lithium ionizes with dissolving at the anode. These ions move across the electrolyte and it is absorbed by a reduction reaction. Free electrons moves along the circuit to supply the current. Because of number of power given to each electron donor atom are known, the number of separated ions can be found with measuring the electrical circuit of the electron. This feature is about specific capacity of the battery, which is mentioned with mA-hour. As an example, a maximum of specific capacity that can accept lithium ions by graphite is reported approximately 372 mAh/g.

Depending on developments in material science, anode, electrolyte and cathode materials can be used for high energy density batteries researches are increasing fastly. As an anode material, despite Si (4000 mAh/g) and SnO_2 (1491 mAg) have high specific capacity, the filling and emptying cycles loses its properties in short period. Nevertheless, if Sn based amorphous oxides prepared by glassy B_2O_3 and P_2O_3, their specific capacity 2-fold higher than conventional lithium ion battery, also shows resistance to the high number of fills and drain cycles. LiO_2 materials with boron as electrolyte material's ionic conductivities are depending between 10^{-3} and 10^{-6} Scm^{-1}. Usually cathodes are composed of transition metal oxides like $LiMO_2$ (M=CO, Ni, Mn). At this point, Li and Co with the amount it found to be limited and expensive in nature are tried to use with low usage it takes effort to reach the maximum capacity. Cathode usage in various ratios as an active material, electrolysis and acetylene black like electrically conductive are improving battery efficiency and decrease usage of expensive materials like Co.

Challenges faced by battery technologies are energy density and ability to cycle. Lead-acid batteries which is used for over a hundred years are fairly heavy (low energy

density) and not safety and before 80 percent of its original capacity, it can make 200 charge-discharge cycles NiCd and Ni-MH batteries are continuously improving over 20 years (Ikeda et al, 1975). These batteries are chosen for high discharge capacity rates, cycle time, price and reliable. Ni-MH cells are using for a long time. It is forecasting that load characteristic of Ni-MH is enough for mass production of hybrid vehicles. However, the main drawback of NiMH batteries is the energy density. A Ni-MH battery pack is too heavy when it is provided for 450 km range in electricity vehicle. The heavy battery is decreasing vehicle's performance in this way. The last improvement of rechargeable battery technology is the components derived from lithium. This is the lightest and most re-active metal. Current progresses are focused on ideal chemical lithium-ion cells and enlarge the anode and cathode surface to improving energy density.

Lithium ion batteries are serving for ease of use like high energy density, high current efficiency, fully loaded capacity and capability of fast charge. These conventional types of batteries contain quickly flammable liquid organic electrolytes. If a cell is damaged by physically, fast charging, fast discharging or it is short-circuited; it may cause to melt quickly. If cells are made from battery packs, the heat generated by the melting of a cell may cause the combustion of the adjacent cells. A suitable cooler and airflow can prevent overheating and melting of cells according to battery packs.

Lithium ion batteries, which are produced by non-flammable solid electrolyte, are more safety and durable in high temperature when compared with liquid electrolyte battery (Steele & Van Gool, 1973). However solid electrolyte battery supply high security, energy densities and performances are lower than liquid electrolyte battery (Di Salvo, Schwall, Geballe, Gamble, & Osiecki, 1971). Recent studies aim high density and strength of the ionic conductivity of the solid electrolyte battery. One-way to improve these properties are producing solid electrolyte as a thin film. Thin film lithium ion batteries have high specific energy, high specific power, high energy efficiency, good performance at high temperatures and low slow discharge features (Hoffart, 2008). They are also quite economical as they are recycled. As a result of theoretical calculations, the thin film battery has two times more energy density than conventional Li-ion battery with capacity of 300 Wh/kg. So there is possibility to store more energy in a smaller space and weight. It can be used in electricity vehicles as an advantage. It also contains chemicals that minimize the impact on the environment. Since there is no memory effect, they require less maintenance than other batteries.

Rechargeable lithium batteries have been developed since the middle of 1980s. In 1991, in response to problems that occur in the cells, Sony declared first lithium-ion battery technology to the consumer market. These improvements are providing two times the energy density for Ni-Cd everyday batteries (Figure2.1). It does not support the discharge voltage than the average cycle. These cells without its obstacles have limited cycle life, low discharge rates and not support safety usage for cell-assisted electronically time in the battery pack assembly. Rapid developments in battery research in the decade has been increased cell capacity more than doubled and to be able to get much more rapid rates of energy. But these batteries contain flammable liquid organic electrolytes and usage area has limited because of their security issues and usage temperatures. The use of non-combustible solid electrolyte in lithium batteries has solved this problem. Solid electrolyte demonstrates high chemical and physical facilities for new generation lithium ion batteries. It also has facilitated the cell design (Murphy & Christian, 1979).

Two types of materials can be used as a solid electrolyte. They are inorganic ceramics and organic polymers. Organic polymers due to low elastic modulus allows the flexible battery production and ceramics which allow production of battery according to high elastic capabilities are more durable and capable of withstanding high temperatures (Murphy & Christian, 1979). Another feature of the batteries is ionic conductivity. Subsequent studies aim to increase the ionic conductivity of solid lithium electrolytes. Studies to increase the ionic conductivity have examined the cathode, anode or electrolyte structure of the battery.

The basis of rechargeable lithium ion battery expresses Li+ cations based on the transfer between the anode and cathode. Very short distance between electrodes able to Li^+ ion transfer easier. This is accomplished by the electrolyte between the electrons produced as a thin film. But so rapid charging and discharging cycles create mechanical stresses on the electrodes. As a result, it leads to cracking of the electrodes and eventually breakup. This is typically used graphite as the anode. Because cathodes semi-porous structure cause lithium intercalation in anode and allow volumetric expansion without structural damage graphite anodes are limited with 372 mAh/g by the capacity of self. Other metals such as aluminum and tin have higher specific capacity. But their smooth and non-porous surfaces do not allow lithium intercalation and the volumetric expansion. Thus prevents the formation of cracks during the charging and discharging cycles and destruction. However, the nano-technology allows building three-dimensional structures on anode surface so this surface allows the development of lithium interpolations. All this

increased surface area of the anode, provides the additional advantage of allowing for the usual high discharge rates.

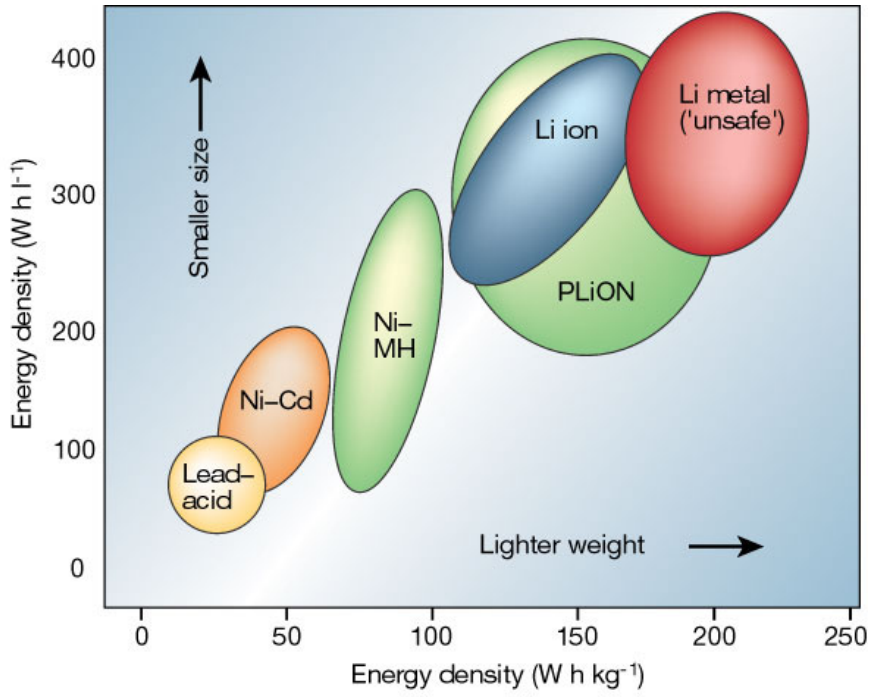

Figure 2. 1. Comprehension of energy density between thin film Li-ion batteries and the other types of batteries (Source: Brohead, 1972).

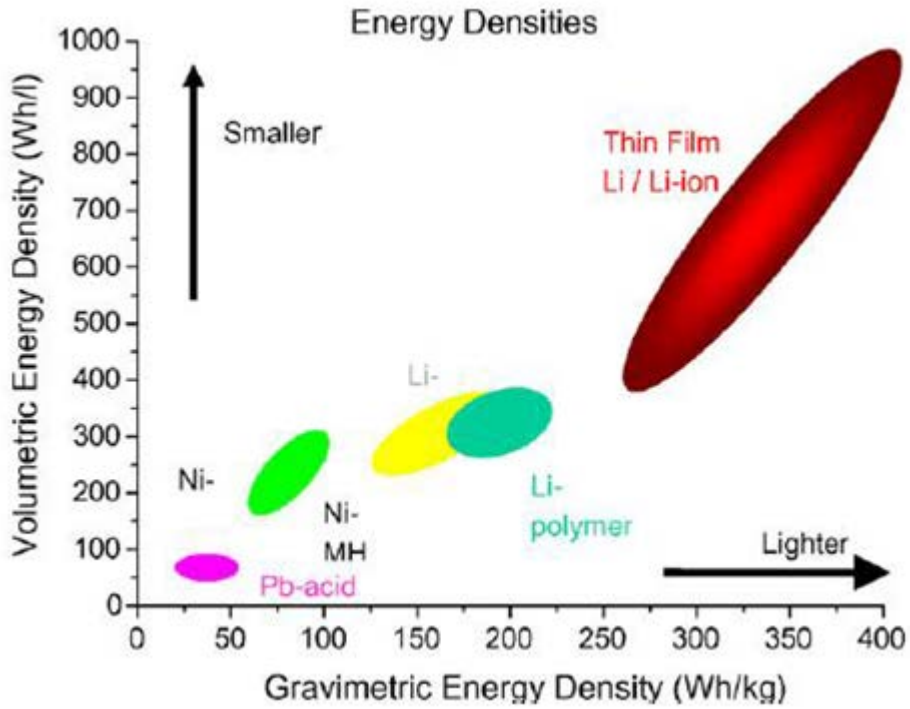

Figure 2. 2. Energy density per unit weight against energy density per unit value for various batteries (Source: Brohead, 1972).

Significant progress also has been in $LiCoO_2$ cathode of lithium ion battery. It offers a high number of cycles of cobalt component and well-featured capacity. However, the production of cobalt is expensive and harmful to the environment. Alternative anode components as $LiNi_{0.5}Mn_{0.5}O_2$ are tested in laboratories and showed high specific capacity and discharge rates. But nickel and manganese have high cost. These cells have not been tested in industrial production facilities (Mizushima, Jones, Wiseman, & Goodenough, 1980). Such materials are applicable for small battery pack located inside the cell phone and laptop. The price of the material in this amount is not significant for the market launch. Electric vehicles will also require the installation of the battery pack into thousands of cells. The price of the material in this application plays a less significant role.

Table 2. 1. Thin film batteries
(Source: Murphy et al, 1972).

Typical thin film batteries

Anode	Electrolyte	Cathode	Voltage (V)	Current ($\mu A/cm^2$)	Capacity
Li	$Li_{3.6}Si_{0.6}P_{0.4}O_4$	TiS_2	2.5	16	45–150 $\mu Ah/cm^2$
Li	$Li_{3.6}Si_{0.6}P_{0.4}O_4$	TiS_2	2.5	16–30	–
Li	$Li_{3.6}Si_{0.6}P_{0.4}O_4$	WO_3–V_2O_5	1.8–2.2	16	60–92 Ah/cm^2
Li	$LiBO_2$	In_2Se_3	1.2	0.1	–
Li	Li_2SO4–Li_2O–B_2O_3	TiS_xO_y	2.6	1–60	40–15 $\mu Ah/cm^2$
Li	Li_2S–SiS_2–P_2S_5	V_2O_5–TeO_2	2.8–3.1	0.5–2	–
LiV_2O_5	LiPON	V_2O_5	3.5–3.6	10	6 $\mu Ah/cm^2$
V_2O_5	LiPON	$LiMn_2O_4$	3.5–1	>2	18 $\mu Ah/cm^2$
Li/LiI	LiI–Li_2S–P_2S_5–P_2O_5	TiS_2	1.8–2.8	300	70 mAh/cm^3
Li	LiBP, LiPON	$LiMn_2O_4$	3.5–4.5	70	100 mAh/g
Li	$Li_{6.1}V_{0.61}Si_{0.39}O_{5.36}$	$MoO_{2.89}$	2.8	20	60 $\mu Ah/cm^2$
Li	$Li_{6.1}V_{0.61}Si_{0.39}O_{5.36}$	$LiMn_2O_4$	3.5–5	10	33.3 $\mu Ah/cm^2$
Li	LiPON	$LiMn_2O_4$	4.5–2.5	2–40	11–81 $\mu Ah/cm^2$
Cu	LiPON	$LiCoO_2$	4.2–3.5	1–5	130 $\mu Ah/cm^2$
Li	LiPON	$LiCoO_2$	4.2–2.0	50–400	35 $\mu Ah/cm^2$
Li	LiPON	$Li_x(Mn_yNi_{1-y})_{2-x}O_2$	4–3.5	1–10	100 mAh/g
Li	LiPON	$LiMn_2O_4$	4–5.3	10	10–30 $\mu Ah/cm^2$
Li	LiPON	Li–V_2O_5	1.5–3	2–40	10–20 $\mu Ah/cm^2$
SiSnON	LiPON	$LiCoO_2$	2.7–4.2	~5000	340–450 mAh/g
Li	LiPON	$LiMn_2O_4$	4.3–3.7	~800	45 $\mu Ah/(cm^2\text{-}\mu m)$
SnO	$Li_{6.1}V_{0.61}Si_{0.39}O_{5.36}$	$LiCoO_2$	2.7–1.5	10–200	4–10 $\mu Ah/cm^2$

Further studies are drawing attention as a promising alternative for $LiFePO_4$ and $LiFeS_2$ development. It is benefiting from low cost facility and non-harmful kind of non-ferrous components. $LiFePO_4$ anode contains less energy density than cobalt. But it is cheaper and easier to manufacture and offers high cycle life. $LiFeS_2$ anodes offer nearly 2 times higher energy density of cobalt. But it has not been fully determined. These two emerging technologies have the potential to reduce the cost of lithium-ion battery production. $LiFePO_4$ cathodes have proven that more thermally stable than $LiCoO_2$, $LiNiO_2$ and $LiMn_2O_4$. Adding potentially safer basic factors prevent leakage of these cells. Laboratory tests have shown that the cycle $LiFePO_4$ particles increased surface area increases the capacity of the cell.

$LiFePO_4$ nano tests represent hopeful results for the surface of the particles. While creating 3-dimensional surface structure, researchers can increase up to 3 times considered to be the ideal limit of the cathode capacity. The study still needs to develop components of the cycle of $LiFePO_4$ nanoparticles. Furthermore nano-particle surface provide research for cheaper and non-toxic alloy cathode.

The first study about thin film lithium ion batteries began in 1982. Same kind of thin film batteries, which were manufactures after 1982, are showed in Figure 2.1. (Kanehori, Matsumoto, Miyauchi, & Kudo, 1983), has produced first thin film battery current density of 16 mA / cm^2 which has TiS_2 cathode, $Li_{3.6}Si_{0.6}P_{0.4}O_4$ electrolyte and lithium ion anode components (Thackeray, David, Bruce, & Goodenough, 1983).

By storing the current density between the anode has reached 100 mA / cm^2 until reaching by electrolysis of lithium thin layer. But the open circuit potential of these cells was limited to 2.8 V. In 1992, Bates et al with using $Li_{3.3}PO_{3.9}N_{0.17}$ (LIPON) solid electrolyte increased batteries open circuit potential to 4.5 Volt (Bates et al., 2000). But there were some limited aspects of LIPON solid electrolyte (Xiong et al., 2011). Inaguma, who have the highest ionic conductivity value so far (10^{-3} S/cm) perovskite to $Li_{0.5}La_{0.5}TiO_3$ (LLTO) has produced solid electrolyte (Figure 2.3) (Inaguma et al., 1993). Where in types purple regions show TiO_3 and yellow and blue regions show Li and La. However, this conductivity value is measured at LLTO's grain. When measured LLTO's total conductivity this value is decreasing 10^{-5} S/cm (Figure 2.5). This is due to prevent grain boundary migration of lithium ions (Murphy & Christian, 1979).

So far the stack form of LLTO has been many studies on the production of solid electrolyte and is calculated for all the different ionic conductivity. These differences arise from different numbers and sizes of LLTO having grain boundaries. In 1998, Katsumata et al with LiNbO3 and in the same year, Chung et al have made the transition metal doped to increase the ionic conductivity of LLTO (Kirino et al, 1986).

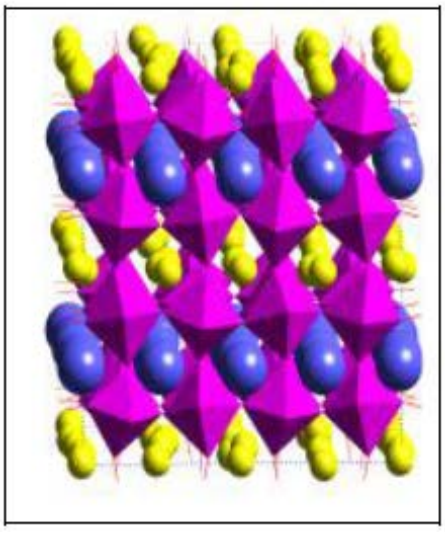

Figure 2. 3. Perovskite crystalline structure of $Li_{0.5}La_{0.5}TiO_3$
(Source: Murphy et al., 1978).

Katsumata et al, in $LiNbO_3$ into different concentrations of Ag and Na metal ossified and transition metal doping concentration increases, they observed an increase in ionic conductivity (Figure 2.4). Produced with doped transition metal-doped $LiNbO_3$ occurs

increase in ionic conductivity because of the lattice parameters of the solid electrolyte is smaller than lattice parameters of $LaLiNbO_3$. Chung et al. has examined the effect of Sn, Zr, Mn, and Ge in LLTO (Chung, Bloking, & Chiang, 2002). Transition metal doped LLTO with ABO_3 perovskite structure effects A-O and B-O's bond strength. Ion contribution has increased bond strength leads to lower anchor. The larger ion additive reduces this force (Kirino, Ito, Miyauchi, & Kudo, 1986). Transition metal doped causes decrease the distance between B-O. Thereby causing an increase in bond strength. Also, it causes lower bond strength between A-O (Kanehori et al., 1983). In 2003, He and colleagues have doped Al to Cr into LLTO (He & Yoo, 2003). The highest total value obtained by doping the ionic conductivity (1.58×10^{-3} S/cm) has achieved (Kelly, Owen, & Steele, 1985). In LLTO, 0.605 Å in diameter Ti^{+4} instead of 0.535 Å in diameter Al^{+3} contribute to decrease between ions and causes an increase of bond strength. By reason of shortening of the distance between Ti and O, the bond strength of them are increasing. But it decreases bond strength between Li and O. Decreasing the bond between Li-O causes decreasing of the activation energy. Also by this perspective, mobility of Li ions increases, and thus causes an increase in ionic conductivity (Kelly et al., 1985).

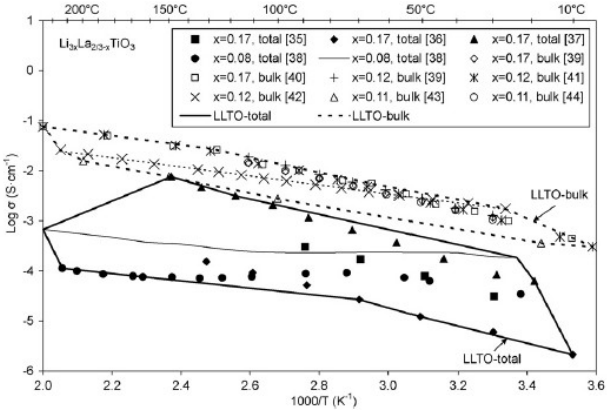

Figure 2. 4. Ionic conductivity of $LaLiNbO_3$ and activation energy (Source: Kanehori et al., 1983).

Ionic conductivities at 300 K and activation energies for $La_xM_yLi_{1-3x-y}NbO_3$ (M = Ag and Na)

	M = Na		M = Ag	
	σ/S·cm^{-1}	E_a/eV	σ/S·cm^{-1}	E_a/eV
$La_{0.25}M_{0.20}Li_{0.05}NbO_3$	2.1×10^{-5}	0.353	3.9×10^{-5}	0.338
$La_{0.20}M_{0.25}Li_{0.15}NbO_3$	5.3×10^{-6}	0.412	2.0×10^{-5}	0.362
$La_{0.15}M_{0.30}Li_{0.25}NbO_3$	2.9×10^{-7}	0.481	2.9×10^{-7}	0.473

Figure 2. 5. Ionic conductivity of LLTO according to Li-La ratio (Source: Murphy and Christian, 1979).

One of the most important achievements of modern materials electrochemistry in recent years is developing of rechargeable lithium-ion battery systems. But just few of them has been successful in commercial market. Li ion batteries, which have many outstanding features, is worked continues to develop these systems. With the production of thin-film battery that has gained speed. Thin film battery system production is possible with anode, solid electrolyte and cathode. Figures 2.6 and 2.7, respectively, illustrate the schematic structure of thin film lithium battery system and produced prototype.

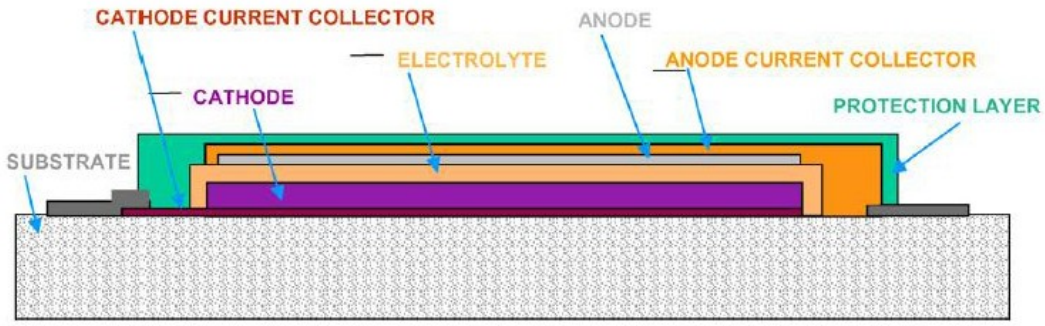

Figure 2. 6. Thin film Li-ion battery schematic representation
(Source: Brohead, 1972).

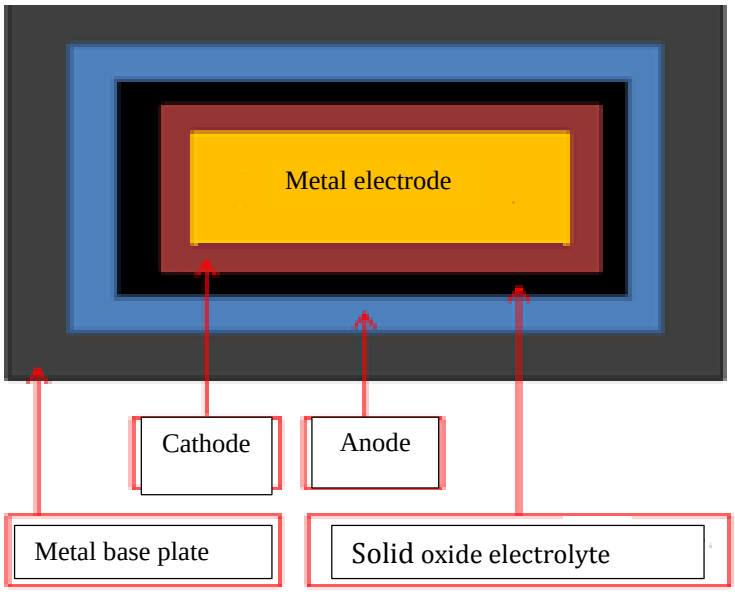

Figure 2. 7. Thin film Li-ion battery prototype.

All components of the cell structure to form a thin film panel (anode, cathode and solid electrolyte) should create an appropriate thin-film production method. Generally, lithium metal is produced by thermal vapor deposition method is used as the anode. The solid electrolyte is produced by cathode and anode is magnetic sputtering (RFMS), chemical vapor deposition (CVD) and electrostatic spray deposition techniques. Lately, especially during, cathode production PLD (pulsed laser deposition) and sol-gel method is used (Rao, Francis, & Christopher, 1977). Recommended by this study, Li-ion cells will be produced which is necessary for the solid electrolyte. As a result of the success of a study, it will be planned with a different project; anode and cathode production will also be performed fully solid-state thin-film battery production.

In 2004, Ahn et al produced 400 nm in thickness of the thin film li0.5la0.5tio3 solid electrolyte on based by Pt / TiO_2 / SiO_2 / Si with PLD method on 500 ºC (Ahn & Yoon, 2004). They found the ionic conductivity for $1.1x10^{-5}$ S/cm. In 2011, Xiong et al produced LLTO thin film with the sputtering method with magnetic base with ITO based (Xiong et al., 2011). They also have studied the optical and electrical properties. They have measured LLTO ionic conductivity of the electrolyte as $5.25x10^{-5}$ S/cm with annealing at 300 °C (Yarascon et al, 2001). In 2012, Ark et al. produced LLTO thin films in different stoichiometry with magnetic sputtering method based on Ar and N_2 atmosphere silicone and stainless steel (Nagaura & Tozawa, 1990). The results of the investigations of the films produced ionic conductivity in both the kind of atmosphere about 10^{-7} S/cm. Increased Li concentration of the compound was observed to decrease the ionic conductivity (Nagaura & Tozawa, 1990). Tan et al. using with the magnetron sputtering method produced LIPON electrolyte with 10^{-6} S/cm ionic conductivity and Li-Al-Ti based (Ohtsuka & Yamaki, 1989). Finally in 2013 Abhilasha et al. LLTO produced by sol-gel method have made a contribution Ag thin film solid electrolyte at different rates (Abhilash, Selvin, Nalini, Nithyadharseni, & Pillai, 2013). They found that the ionic conductivity increases in grain and grain boundaries within the structure by increasing the contribution of Ag (Table 2.2) (Ohtsuka & Yamaki, 1989).

Table 2. 2. Ionic conductivity of Ag doped LLTO.
(Source: Naguara and Tozawa, 1990).

Samples	Grain conductivity ($S\,cm^{-1}$)	Grain boundary conductivity ($S\,cm^{-1}$)
$Li_{0.5}La_{0.5}TiO_3$	1.41×10^{-3}	1.875×10^{-4}
$Ag_{0.1}Li_{0.4}La_{0.5}TiO_3$	2.77×10^{-4}	1.404×10^{-5}
$Ag_{0.3}Li_{0.2}La_{0.5}TiO_3$	6.033×10^{-4}	2.907×10^{-6}
$Ag_{0.5}La_{0.5}TiO_3$	1.166×10^{-3}	1.3766×10^{-3}

The aim of this study is to produce solid-state electrolyte, which can be used in all solid-state thin film Li-ion battery. An important point for solid electrolyte material is LLTO, which is used for production of li-ion batteries. As a result explosion and yield problems of the electrolyte at high temperatures along with a high load capacity of the battery will be eliminated.

There are two ways will be monitored to increase the high ionic conductivity in the battery. In the first method, LLTO thin film electrolytes with magnetic sputtering method (Whittingham, 1976) by heating substrate while producing crystallization increased and grain boundaries are reduced. In the second method, LLTO thin film is doped by different amounts of aluminum. In addition, it is tried to increase the ionic conductivity with rise in lithium ion density with caused by ionic radius decrease.

CHAPTER 3

EXPERIMENTAL PROCEDURE

Two steps as target preparation and thin film growth are composed in experimental set-up. Initially to use in RF magnetron sputtering system an appropriate shaped target, which can be fixed in the sputter gun is needed. Secondly thin films are grown by RF magnetron sputtering system while the substrate has been heated by approximately 220 ^{o}C. After the LLTO and Al-doped LLTAlO thin film samples are grown with suitable deposition parameters the characterization analyses part is examined by optical, structural and electrical aspect respectively. But just before the experimental procedure there is brief information about mechanism of thin films and thin film deposition techniques at the beginning of this chapter.

3.1. Mechanism and Physics Behind of Thin Films

Thin film is a layer that on a chosen substrate, which has approximately from a few nanometers to a ten-micrometer thickness (Krishina, 2002). In last few decays thin film applications spread out to variety of technological areas rapidly. While, it is applicable for medical, military, communication, and transportation industries, also convenient for everyday life tools.

Thin film technology is one of the main utilizing application areas for integrated circuit industry. One of the paramount facilities is that, the cost of thin film growth is cheaper corresponding to bulk materials. To apply this useful technology to sort of

sensors, energy generation, microchips, optical-devices and electronic displays is low cost and shows appreciate design.

The required microelectronic devices, which have higher qualities than the conventional ones, are needed to the new kind of thin film growth techniques. For this reason lots physical and chemical studies focus on thin film structure, thin film characterization and the growth techniques.

As can be seen in Figure 3.1 essentially nano-structural thin films are not only growth in vacuum processing systems but also growth in non-vacuum system. However for ascendant quality thin films, high vacuum atmosphere is most desired condition. All the thin film growth techniques are occurred by not only chemical or not only physical composition, it is a great combination of the both physical and chemical reactions.

3.1.1. Thin Film Growth Techniques

Thin film applications are based on physical, optical and electrical properties of the appropriate material. All these properties are subjected to the growth techniques. To investigate the physics behind of thin films the best way to classify the generation techniques and look at film qualities beside the procedure as can be seen in Figure 3.1. In this perspective initially thin film growth techniques are branched as vacuum media processes and non-vacuum media processes. Vacuum media processes are mostly preferred due to high quality of the films for laboratories or industries.

3.1.2. Vacuum Media Process

Vacuum media process mainly consists of physical vapor deposition (PVD) and chemical vapor deposition (CVD). In PVD process, the vapored particles are induced through the substrate surface from a resource by physical reactions such as evaporation and sputtering. There are some requirements to growth thin film by PVD. First of all a vacuum media must be ready which is formed by a vacuum chamber, valve, gas vents, flanges, o-rings. After a complete vacuum chamber there must be mechanic and turbo pumps (alternatively ion or diffusion pumps etc.). Also to get information about the vacuum value of the chamber and to control the gas amount, vacuum gauges must be integrated to the system. In additionally, the gas tubes must be connected to send preferred

gas. Finally a determined substrate is placed to the sample holder and a target is placed to the sputter gun as a source.

3.1.2.1. Sputtering Techniques

Sputtering mechanism can be explained basically as, the surface of the target is hit with particles which have high kinetic energy so the surface atoms are thrown out. Physically there are ion-surface interaction plays an important role. The target surface is behaved as cathode which is bombarded by positive ions.

$$Ar + e^- \longrightarrow Ar^+ + e^- + e^- \qquad (3.1)$$

But there are no positive ions in vacuum chamber at the beginning of the process. Because the used inert gas (generally using argon gas) is ionized as can be seen in Eq. 3.1.

The required minimum energy to remove an atom from the target surface is called threshold energy (E_o). For constitute of sputtering E_0 is must be higher than the surface binding energy of the target atoms. To reach higher sputtering rate while the electrons are moving, magnetic field as parallel to target surface is applied to cause much ionization. It is named as magnetron sputtering deposition.

To determine the quality of deposition one of the serious points is sputtering yield. It is the number of sputtering atoms, which is thrown out from the target surface per circumstance ions.

In this study high vacuum RF (radio frequency) magnetron sputtering technique was used. Deposition parameters are shown in Table 3.2, 3.3, 3.4 and 3.5 clearly. RF magnetron sputtering is preferred for ceramic or insulator targets. Because, the RF area pulsation rises the ionization ratio. While DC sputtering electric field is directing the excited ions through the cathode surface, RF sputtering electrodes fluctuates by applied alternating current. RF loops generate capacitive pairings and the other electrons are advocated at cathode area smoothly.

3.1.2.2. Evaporation Techniques

Numerous kinds of materials can be evaporated and growth a thin film layered on a chosen substrate surface. Evaporation temperature is tunable sensitively to generate films with minimum contamination. To get rid of impurities the evaporating material should have disregarded vapor deposition pressure and decomposition temperature of the process temperature.

There are two kinds of evaporation techniques are used widely as thermal and electron beam evaporation. In thermal evaporation systems a solid source material is heated in vacuum till the temperature reaches to a value, which produces a vapor pressure. This evaporated particles of the source material, heat the substrate and glued to this surface so thin film coating is occurred.

Secondly, the source is hit by electron beam and the solid particles change the phase from solid to gas. After that, the atoms participate into solid phase and thin film layer is produced.

Mainly there are two kinds of evaporation techniques are used in common such as thermal, ion-beam. But, alternatively ion plating evaporation and laser ablation evaporation techniques are also using to deposit thin films.

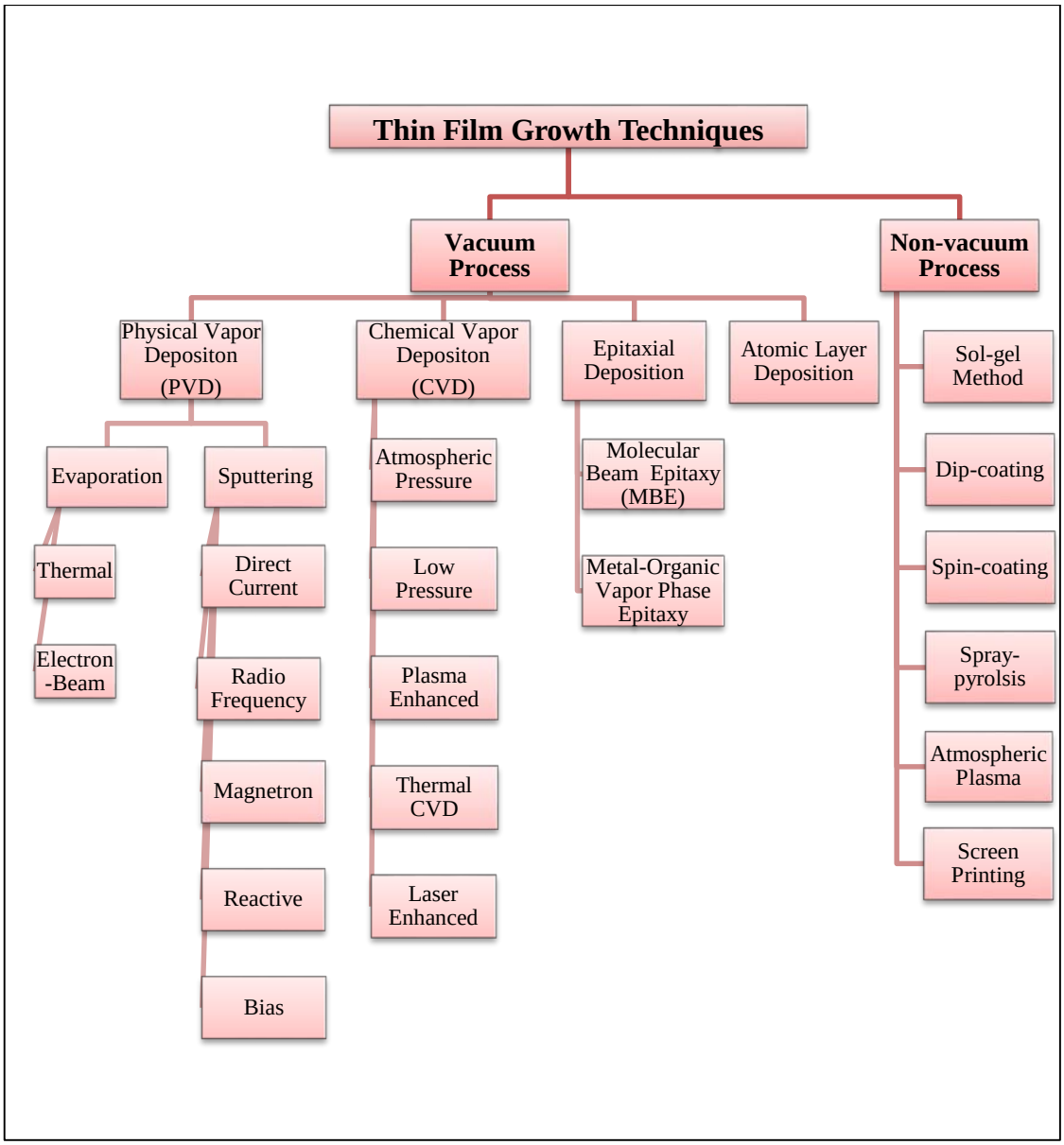

Figure 3. 1 Thin film deposition techniques.

3.2. Target Preparation

In this study 4 targets are produced as pure LLTO target and the Al-doped $Li_{0.5}La_{0.5}Ti_{1-x}Al_xO_3$ (LLTAlO) targets with the amount of x=0.05, 0.10, 0.15 to compare Al-doping effect on structure and ionic conductivity of the synthesized samples. Beginning of the story the appropriate target value, which can be fixed with the deposition gun of RF magnetron sputter system, was determined as seen in Figure 3.1.

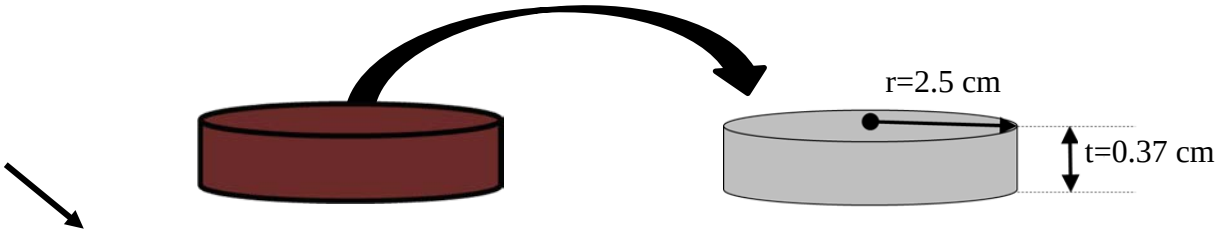

Figure 3. 2. LLTO Target in Cupper base-plate

3.2.1. Pure (LLTO) Target Preparation

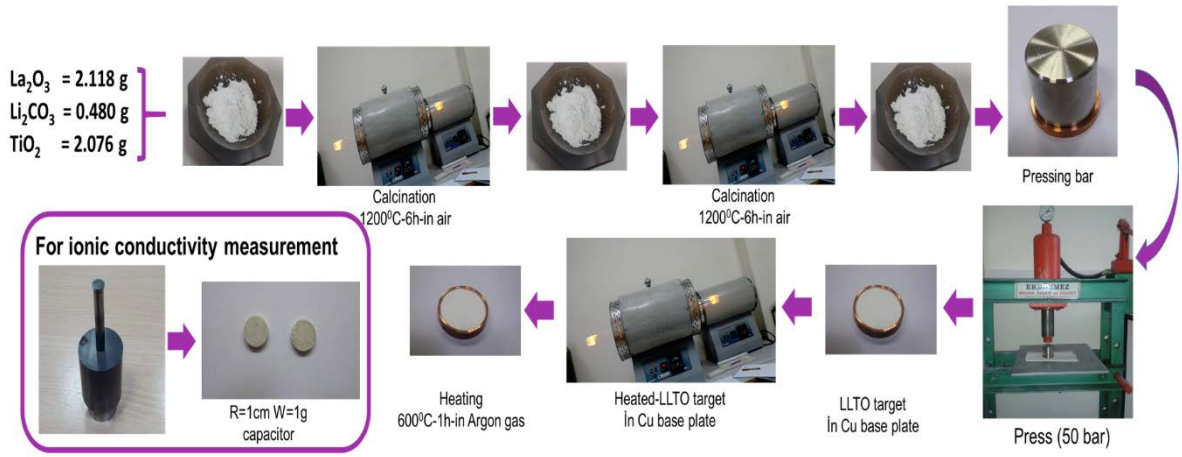

Figure 3. 3 Pure-LLTO target preparation procedure

Pure-LLTO target preparation procedure which is summarized in Figure 3.2, explained step by step below.

- Initially the appropriate chemical reaction equation is composed.

$$La_2O_3 + Li_2CO_3 + TiO_2 \longrightarrow Li_{0.5}La_{0.5}TiO_3 + CO_2 \qquad (3.2)$$

- To obtain 1 mole $Li_{0.5}La_{0.5}TiO_3$ (LLTO),

  0.25 mole La_2O_3=2.118 g

  0.25 mole Li_2CO_3 =0.480 g and

  1.00 mole TiO_2 =2.076 g

  Powders, which have 99.999% purity, are mixed in agate mortar.

- The mixture of the powder is grinded approximately 6 hours in agate mortar, to obtain a homogeny distribution, and then taken to the crucible to start the first calcination at 1200^{o}C for 6 hours in air atmosphere.
- The calcined powder is grinded again and the second calcination at 1200^{o}C for 6 hours in air atmosphere is applied.
- The calcined powder is pressed into Cu-base plate, which is suitable for our sputtering system gun, by 5 MPa with a press button as shown in Figure 3.2.
- Finally, the disk-shaped LLTO target in Cu base-plate is heated at 600^{o}C for an hour in air atmosphere to get more compact target.

3.2.2. Al-Doped LLTAlO Targets Preparation

To observe doping effect on LLTO targets and thin films first of all the suitable doping rates are searched. Especially most of recent researches indicate that small amounts of Al_2O_3 increasing the ionic conductivity performance for LLTO electrolyte (ref.1-2). Based on these studies, for Al-doped $La_{0.5}Li_{0.5}Ti_{1-x}Al_xO_3$ target the stoichiometric rates are determined as x=0.05, x=0.10, x=0.15.

Table 3. 1. Al_2O_3 doping amounts

Target	Al_2O_3 doping amounts
LLTO-pure	0
LLTAlO-0.05	0.05
LLTAlO-0.10	0.10
LLTAlO-0.15	0.15

For doping procedure all the steps are similar with the pure one. The first 4 steps are applied in the same way but after the second calcination appropriate amount of Al_2O_3 is doped into the mixture of powders and the calcination is started at 1200 ^{o}C for 6 hours in air atmosphere.

Previously Al-doped LLTAlO powder is calcined again at 1200 ^{o}C for 6 hours in air atmosphere and the next steps are continued like the pure targets. Predictably the calcined powder is grounded to the Cu-base plate and pressed with the cylindrical press button by 5 MPa. Finally heat treatment is applied to the disk-shaped LLTAlO target at

600ºC for an hour in air atmosphere. All these Al-doping process is demonstrated with the Figure 3.3 clearly.

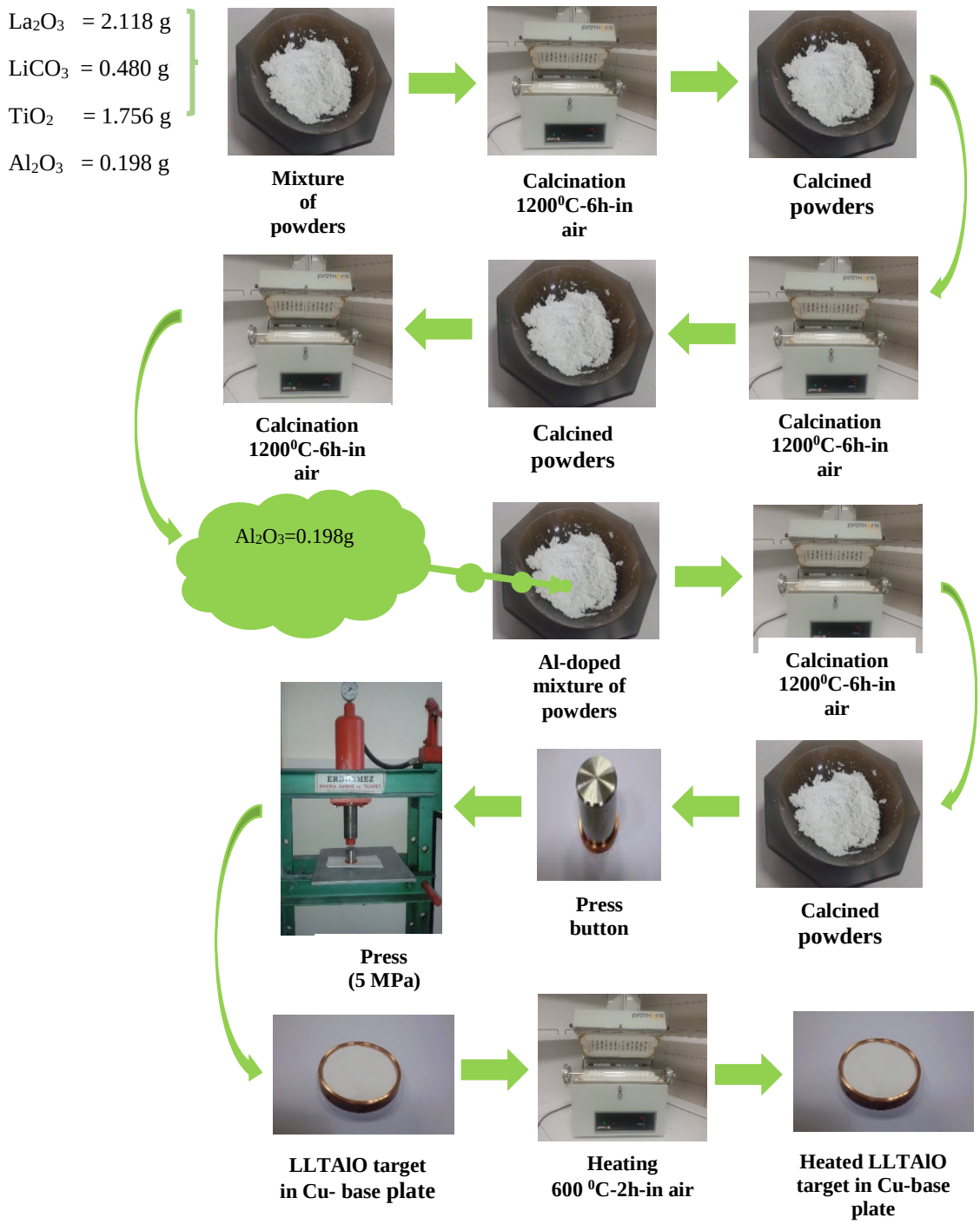

Figure 3. 4. Al-doping process.

3.3. Thin Film Fabrication

In this study pure and Al-doped LLTO thin films are produced by high vacuum RF (Radio Frequency) magnetron sputtering technique. As a substrate, Soda Lime Glass (SLG) was used for optical, structural characterization and ITO coated SLG was used for ionic conductivity measurement.

The SLG, which is used as a substrate, must be clean before grounded to the system. For cleaning procedure firstly the SLG is ultrasonically cleaned in acetone, after than propanol for 10 minutes. ITO coated SLG is just cleaned by precision wipes with acetone.

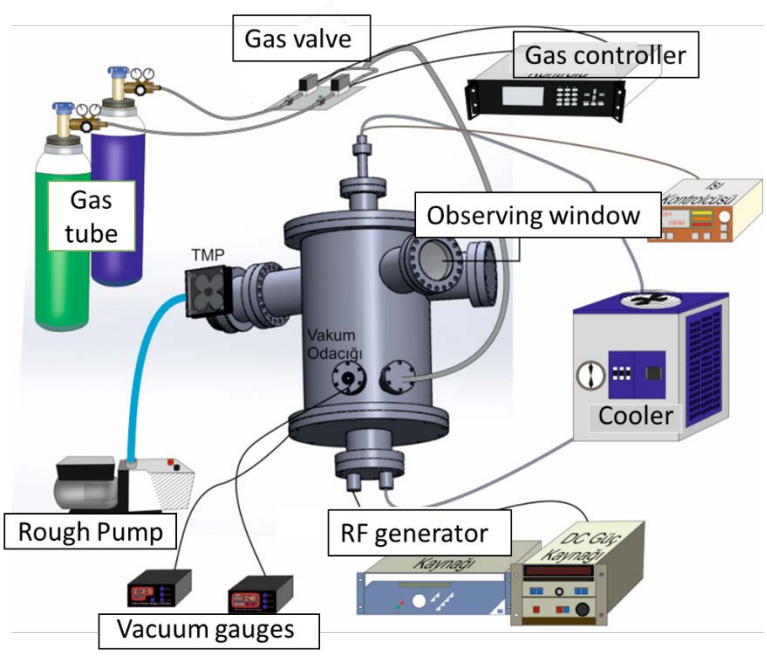

Figure 3. 5. RF magnetron sputtering system.

The RF magnetron sputtering system was firstly vacuumed by rough pump and then the turbo molecular pump till the vacuum range reach to 10^{-6} Torr which is the ideal value of high vacuum thin film deposition. While depositing the thin film the substrate is heated approximately 220 ^{o}C to increase the grain boundaries (Nong et al., 2015). The heating holder of our sputtering system can be seen in Figure 3.6.

Figure 3. 6. Heating holder of the RF magnetron sputtering system.

Before deposition, pre-sputtering is started for 10 minutes to get rid of contaminants of the target. During the deposition 50 sccm Argon gas is sent to the chamber while the working pressure is around 10^{-3} Torr. While the RF power supplier performs 102 W forward power (FWDP), approximately 12 W reflected power (REFP) occurs so the applied sputtering power is around 90 W. Deposition periods are determined as 15, 30, 60, 90 minutes to compare the effects of the film thickness on optical, structural, electrical properties.

When the deposition process is completed the thin films are annealed in air at 100 ^{o}C, 200 ^{o}C, 300 ^{o}C, 400 ^{o}C for 2 hours (Xiong et al., 2011). The annealed films are growth on ITO coated SLG for 60 minutes. Deposition parameters and film thicknesses are shown for each used targets separately in Table 3.2, 3.3, 3.4, 3.5.

Figure 3. 7 Cross-section of layered structure of LLTO thin film.

Table 3. 2. Deposition parameters and film thicknesses of LLTO_pure target

Sample name	Target	Substrate	Gas (Ar) (sccm)	RF		T (^oC)	Deposition period (min)	Film thickness (nm)
				FWDP (W)	REFP (W)			
SG.1	LLTO_ pure	SLG	50	130	10	224	30	77.5
SG.2	LLTO_ pure	SLG	50	130	11	273	30	86
SG.3	LLTO_ pure	SLG	50	100	5	240	30	83
SG.4	LLTO_ pure	SLG	50	90	3	287	30	80
SG.5	LLTO_ pure	SLG	50	102	7	220	60	140
SG.33	LLTO_ pure	ITO	50	102	7	215	90	35
SG.34	LLTO_ pure	ITO	50	102	9	210	60	85
SG.35	LLTO_ pure	ITO	50	102	9	210	30	144
SG.36 (for anneal)	LLTO_ pure	ITO	50	102	9	210	15	24
SG.37 (for anneal)	LLTO_ pure	ITO	50	102	9	210	60	110
SG.38 (for anneal)	LLTO_ pure	ITO	50	102	9	210	60	88
SG.39 (for anneal)	LLTO_ pure	ITO	50	102	9	210	60	102
SG.40 (for anneal)	LLTO_ pure	ITO	50	102	10	210	60	101

Table 3. 3. Deposition parameters and film thicknesses of LLTAlO_1 x=0.05 target

Sample name	Target	Substrate	Gas (Ar) (sccm)	RF		T (^oC)	Deposition period (min)	Film thickness (nm)
				FWDP (W)	REFP (W)			
SG.6	LLTAlO-1 x=0.05	SLG	50	102	12	220	60	155
SG.7	LLTAlO-1 x=0.05	SLG	50	102	12	220	30	85
SG.8	LLTAlO-1 x=0.05	ITO	50	102	12	220	30	75
SG.43	LLTAlO-1 x=0.05	ITO	50	102	9	210	60	XXX
SG.44 (for anneal)	LLTAlO-1 x=0.05	ITO	50	102	10	210	60	96
SG.45 (for anneal)	LLTAlO-1 x=0.05	ITO	50	102	12	210	60	100
SG.46 (for anneal)	LLTAlO-1 x=0.05	ITO	50	102	11	210	60	XXX
SG.47 (for anneal)	LLTAlO-1 x=0.05	ITO	50	102	11	210	60	XXX
SG.48	LLTAlO-1 x=0.05	SLG	50	102	11	200	90	138
SG.49	LLTAlO-1 x=0.05	ITO	50	102	10	200	15	65
SG.50	LLTAlO-1 x=0.05	ITO	50	102	10	200	60	XXX

Table 3. 4. Deposition parameters and film thicknesses of LLTAlO_2 x=0.10 target

Sample name	Target	Substrate	Gas (Ar) (sccm)	RF		T (^oC)	Deposition period (min)	Film thickness (nm)
				FWDP (W)	REFP (W)			
SG.09	LLTAlO-2 x=0.10	SLG	50	102	10	220	60	116
SG.10	LLTAlO-2 x=0.10	SLG	50	102	9	220	90	226
SG.11	LLTAlO-2 x=0.10	ITO	50	100	9	220	60	125
SG.12	LLTAlO-2 x=0.10	ITO	50	107	10	220	90	190
SG.13	LLTAlO-2 x=0.10	ITO	50	107	9	220	30	62
SG.14	LLTAlO-2 x=0.10	ITO	50	107	9	220	15	25
SG.15	LLTAlO-2 x=0.10	SLG	50	102	7	220	30	63
SG.16	LLTAlO-2 x=0.10	SLG	50	102	7	220	15	30

Table 3. 5. Deposition parameters and film thicknesses of LLTAlO_3 x=0.15 target

Sample name	Target	Substrate	Gas (Ar) (sccm)	RF		T (°C)	Deposition period (min)	Film thickness (nm)
				FWDP (W)	REFP (W)			
SG.17	LLTAlO-3 x=0.15	SLG	50	102	7	220	60	120
SG.18	LLTAlO-3 x=0.15	SLG	50	102	6	220	90	233
SG.19	LLTAlO-3 x=0.15	SLG	50	102	6	220	30	74
SG.20	LLTAlO-3 x=0.15	SLG	50	102	6	220	15	35
SG.21	LLTAlO-3 x=0.15	ITO	50	102	6	217	90	216
SG.22	LLTAlO-3 x=0.15	ITO	50	102	5	213	60	118
SG.23	LLTAlO-3 x=0.15	ITO	50	102	5	215	30	43
SG.24	LLTAlO-3 x=0.15	ITO	50	102	5	214	15	24
SG.25	LLTAlO-3 x=0.15	ITO	50	102	6	210	60	131
SG.27	LLTAlO-3 x=0.15	ITO	50	102	6	210	60	135
SG.29	LLTAlO-3 x=0.15	ITO	50	102	6	210	60	127
SG.30	LLTAlO-3 x=0.15	ITO	50	102	6	210	60	155
SG.31	LLTAlO-3 x=0.15	ITO	50	102	5	210	30	63
SG.32	LLTAlO-3 x=0.15	ITO	50	102	5	210	15	29

CHAPTER 4

RESULTS AND DISCUSSION

4.1. XRD Analyses of Targets

The crystal phases in pure and Al-doped LLTO targets were examined by X-ray diffraction method. The crystal structure of the targets was characterized by Bruker D8 Discover X-ray diffractometer (XRD) over the angular range $20^o < 2\theta < 80^o$. The peaks of the powders are observed as $2\Theta = 32.8^o$, 40.30^o, 47.00^o, 58.40^o, 68.60^o, 78.10^o and 29.30^o. Cubic LLTO phase planes are identified as (110), (112), (200), (212), (220), (310) and (101) by JCPDS 89-4928 card number and the results are definitely compatible with the literature. Since the mass of doped Al_2O_3 is less than the total target mass, the Al_2O_3 peak cannot be seen in XRD analysis. It can be clearly seen in Figure 3.4 that, Al-doping process increases the crystallization.

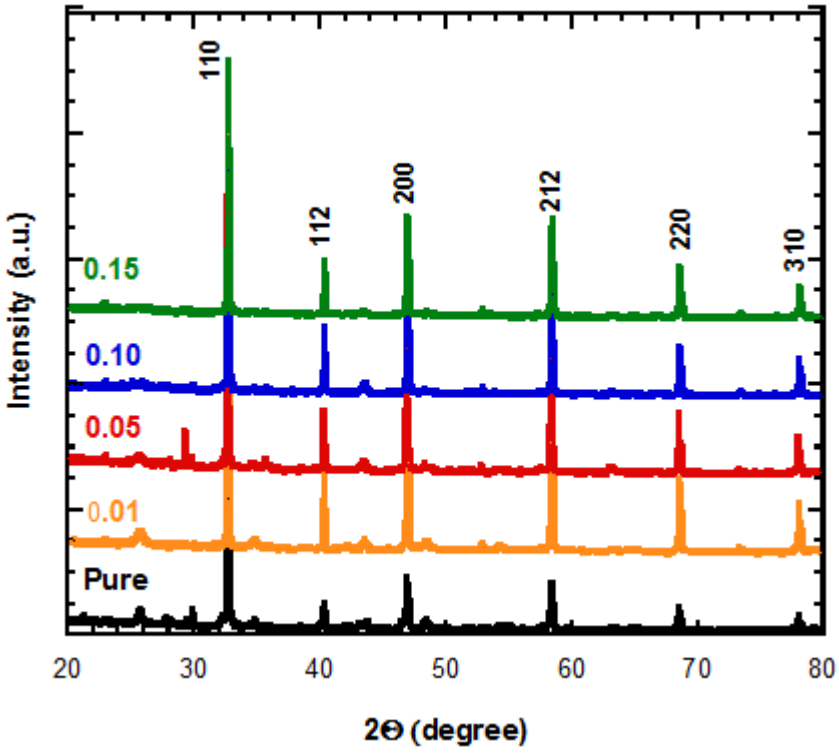

Figure 4. 1. XRD patterns of pure-LLTO and different amount of Al-doped LLTAlO targets.

4.2. Raman Analyses of Targets

In this study, Raman spectroscopy analyses of pure and Al-doped targets were measured by confocal Raman microscopy with green laser, which has 488 nm wavelengths to determine the phase structure. Figure 3.5 shows (a) the pure_LLTO, (b) Al-doped LLTAlO x=0.05, (c) Al-doped LLTAlO x=0.10 and (d) Al-doped LLTAlO x=0.15 diffraction peaks. 144, 234, 317, 530 cm^{-1} bands consist on the literature respectively (Antoniassi, González, Fernandes, & Graeff, 2011). 144 and 317 cm^{-1} peaks are attributed to in plane and c axis titanium vibration modes likewise the 234, 529 cm^{-1} peaks are referred by oxygen (Sanjuán, Laguna, Várez, & Sanz, 2004).

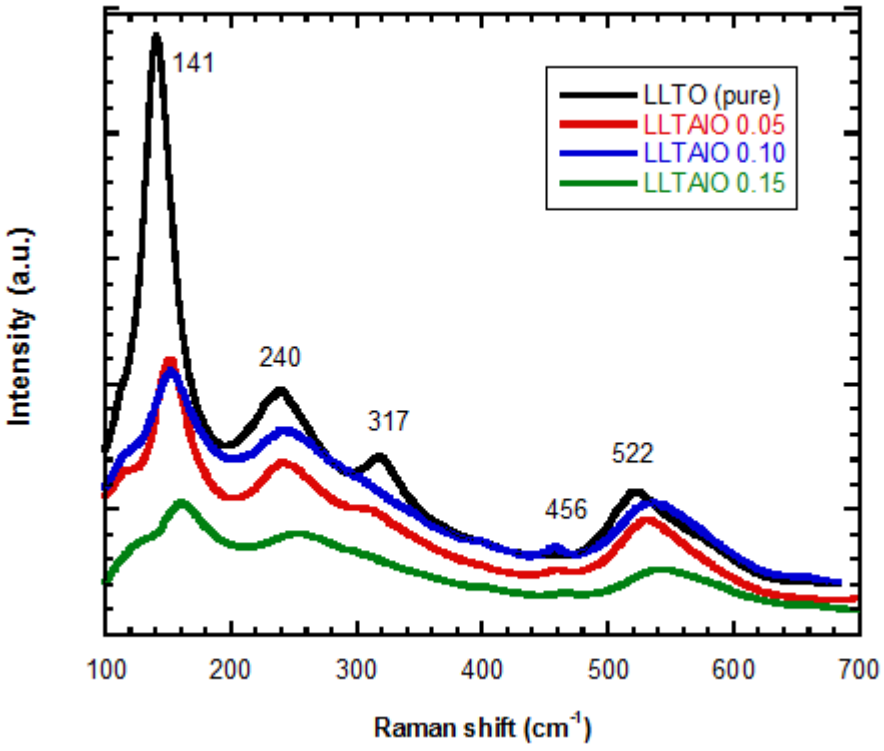

Figure 4. 2. Raman spectra of pure, x=0.05, 0.10, 0.15 LLTAlO targets.

4.3. Thin Film Characterization

Pure and Al-doped LLTO thin films were growth by appropriate deposition parameters and characterized by Raman spectroscopy, XRD, SEM analyses. After the structural analyses according to bonding energy position of the elements on the thin film surface, chemical compositions were investigated by X-ray photoelectron spectroscopy

(XPS). Subsequently for ionic conductivity measurement aluminum was evaporated in vacuum to the thin film surface and then got contact by prop station.

4.3.1. XRD Analyses

When the pure and Al-doped LLTO thin films were analyzed by X-ray diffraction between $2\Theta=20^{o}$-80^{o} and 0.04 ^{o} /sec scan rate, it was seen that the films have amorphous structure as shown in Figure 4.3.

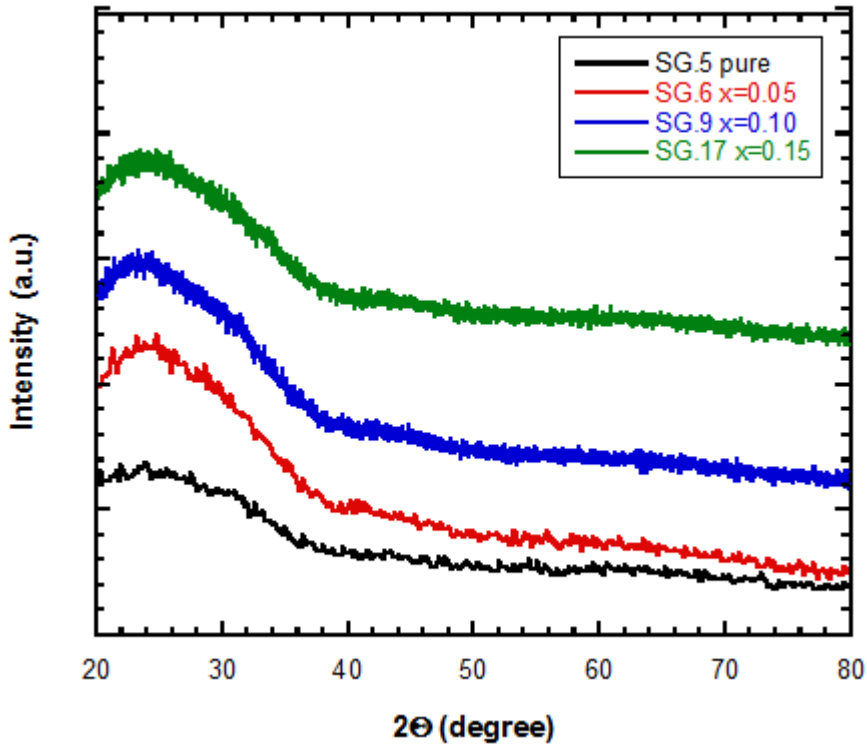

Figure 4. 3. XRD patterns of pure and x=0.05, 0.10, 0.15 Al-doped LLTO thin film.

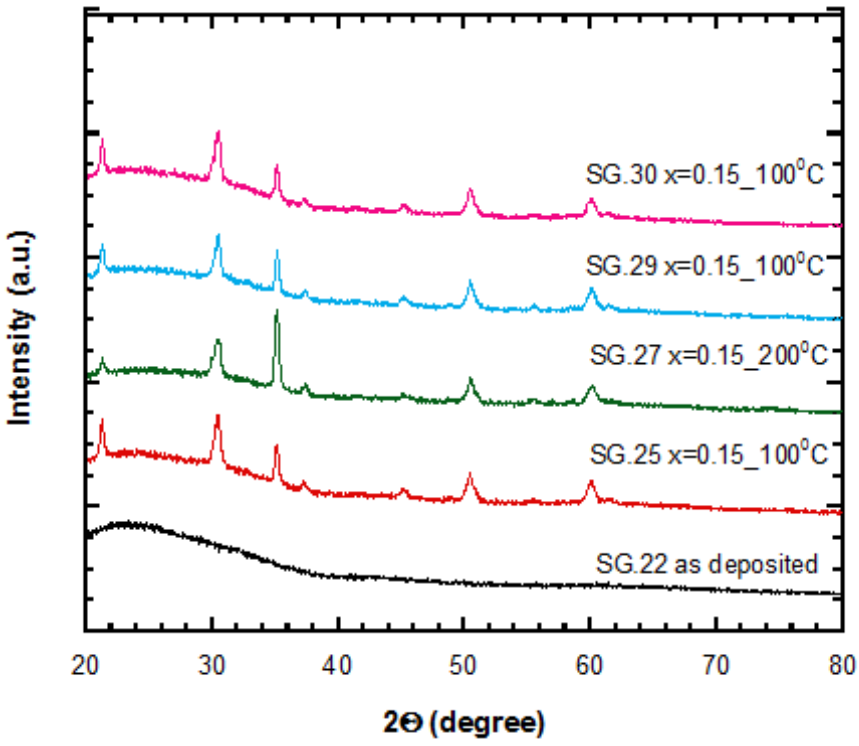

Figure 4. 4. XRD patterns of x=0.15 Al-doped LLTO thin films on ITO substrate annealed at various temperatures.

Samples SG.22, 25, 27, 29 and 30 were deposited with x=0.15 Al-doped LLTAlO target at 50 sccm Ar gas atmosphere by approximately 100 W RF power, for 60 minutes. After thin film deposition the films are annealed at 100 ^{o}C, 200 ^{o}C, 300 ^{o}C, 400 ^{o}C in air atmosphere for 2 hours.

In literature while the best ionic conductivity of thin film electrolytes have amorphous structure, some of the studies show that if the crystallization increases the ionic conductivity ascends as well. The reason of the high ionic conductivity of amorphous structured films, there is not grain boundary like crystalline structured ones and when the annealing temperature increases, the surface roughness goes up. Otherwise Xiong et al show that grain boundary increases by annealing temperature. While the boundary thickness is decreasing the ionic conductivity is rising (Xiong et al., 2011).

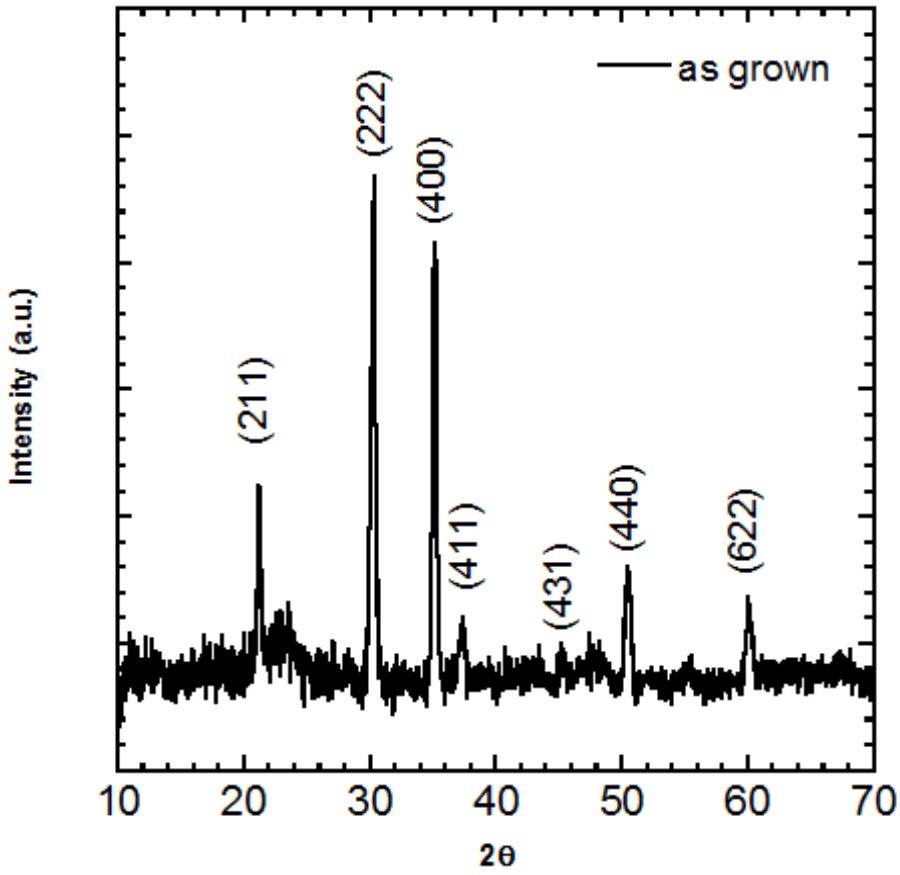

Figure 4. 5. XRD pattern of ITO thin film as used substrate
(Source: Koseoglu et al., 2015)

Annealed thin films have 2θ =21, 30, 35, 51 and 60^{o} peaks. These peaks correspond to (211), (222), (400), (440) and (622) planes of ITO as shown in Figure 3.7. For this reason the obtained peaks are coming from the ITO substrate which is used for electrical measurement.

4.3.2. Optical Analyses

Electrochromic devices show similarities due to material and operation with thin film Li-ion batteries. These kinds of devices have large application area like medical devices as smart cards, detectors, neurotransmitters in addition to micro electromechanical systems (Xiong et al., 2011).

Al doped LLTO electrolyte material is that studied in this thesis has wide range of usage area due to its high electrochemical stability and Li-ion conductivity. Because the thin film electrolytes, which are growth by RF magnetron sputtering technique, have

larger grain boundaries (Li et al., 2006). To analyze the optical properties of the LLTO thin films, Perkin Elmer UV Visible Spectrophotometer instrument is used.

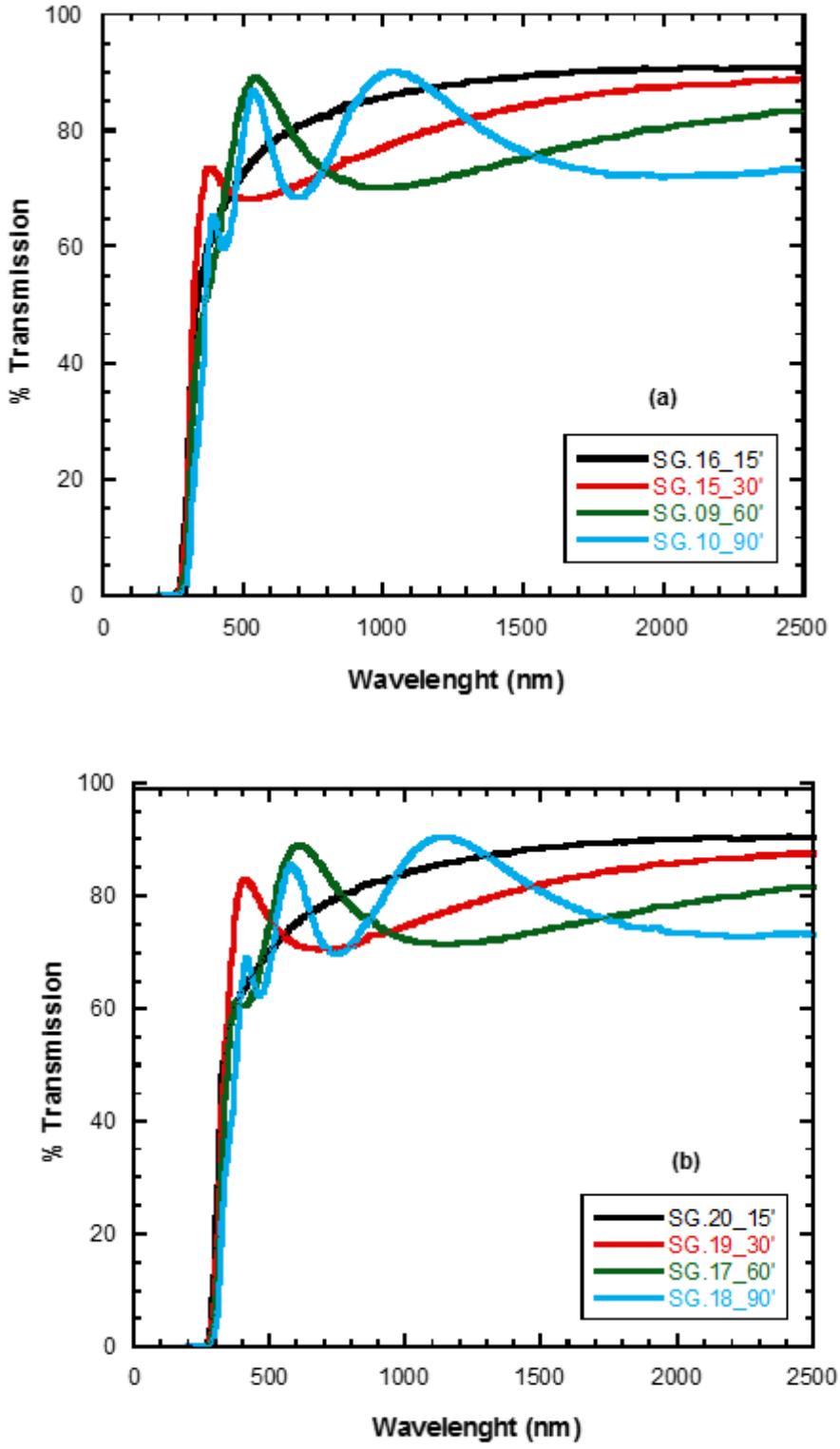

Figure 4. 6. (a) Transmission spectra of x=0.10 Al-doped LLTO thin films.
(b) Transmission spectra of x=0.15 Al-doped LLTO thin films.

Figure 4.5 (a) shows the transmission spectra of x=0.10 Al-doped LLTO thin films on SLG substrate which were growth for 15, 30, 60, 90 minute deposition periods and similarly Figure 4.5 (b) shows the transmission spectra of x=0.15 Al-doped LLTO thin films which have the same deposition period. In this analyze effect of thickness on transmission is determined by changing the deposition period.

Figure 4.6 shows the transmission spectra of pure and Al-doped thin films on SLG and it can be seen that optical transmission of all the samples, which have different Al-doping rates is approximately 75 %. This property satisfies optical transmission condition of electrolyte layer (Xiong et al., 2011).

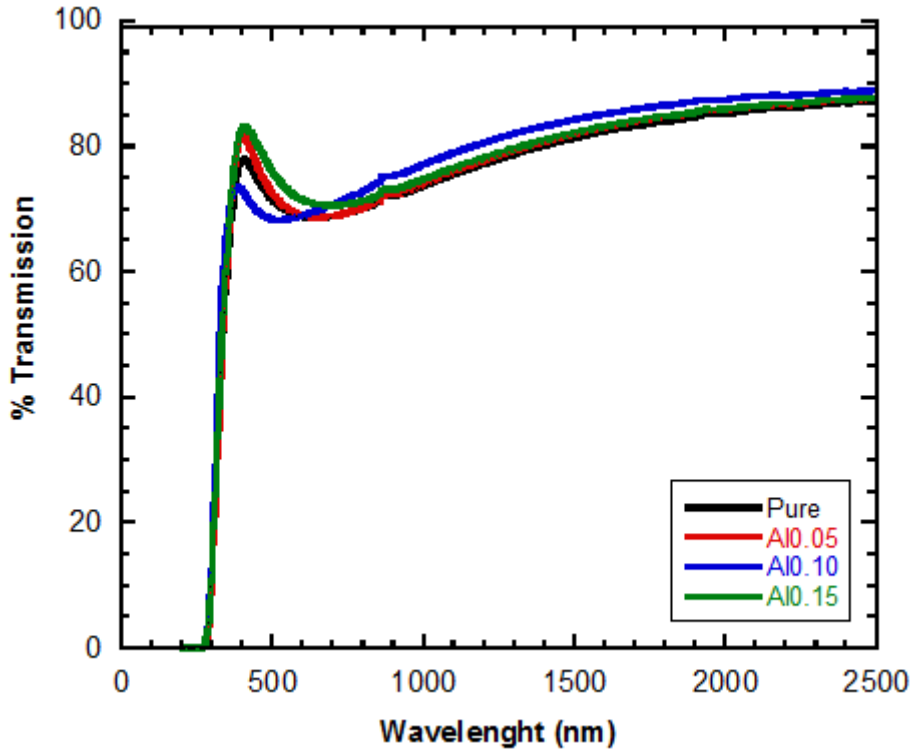

Figure 4. 7. Optical transmission spectra of pure and x=0.05, 0.10, 0.15 Al-doped LLTO thin films.

4.3.3. XPS Analyses

Chemical composition of the thin films was investigated by SPECS X-ray Photoelectron Spectroscopy (XPS) instrument with C 1s (284.6 eV) bonding energy calibration due to bonding energy position of the surface elements.

Figure 4.7. shows the XPS survey spectra of x=0.05, 0.10, 0.15 Al-doped LLTAlO thin films. It is seen that from this graph, the films are composed by lanthanum, oxygen,

titanium, carbon, aluminum and lithium. The result of this analyses correspond to the literature (Chen et al., 2012). During the measurement, focused on La 3d and Ti 2p regions.

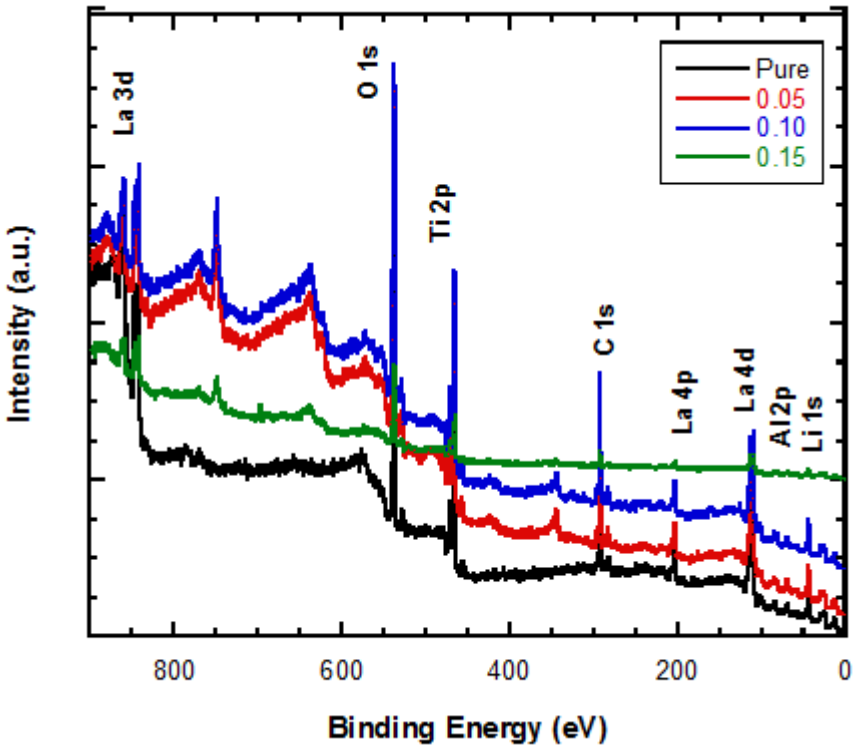

Figure 4. 8. XPS survey spectra of various Al-doped LLTAlO thin films.

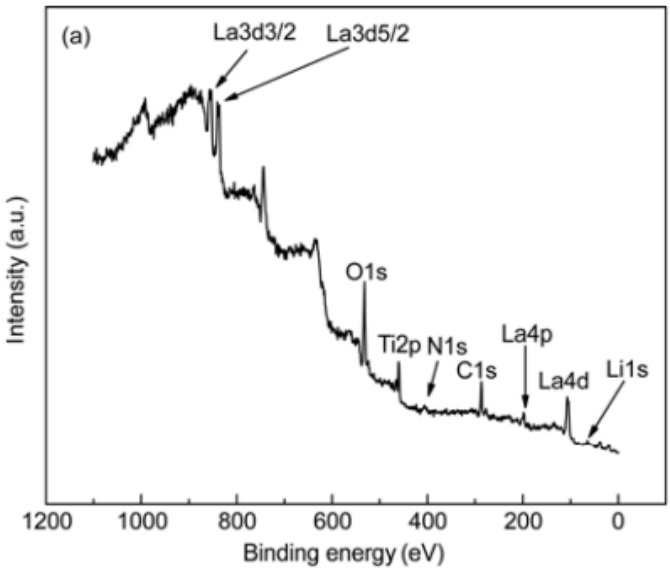

Figure 4. 9. XPS survey spectra of LLTO thin film
Source: (Chen et al., 2012)

Figure 4.9 shows XPS La 3d spectra of the thin films, which are deposited 30 minutes by RF magnetron, sputter system. The films reveal 855.2 and 850.6 eV bonding energy peaks which are correspond to La $3d_{3/2}$ coupling meanwhile 838.3 and 833.7 eV bonding energy peaks are correspond to La $3d_{5/2}$ (Li et al., 2006). La $3d_{5/2}$ spin orbit separation has 4.6 eV distinction matches up with the literature.

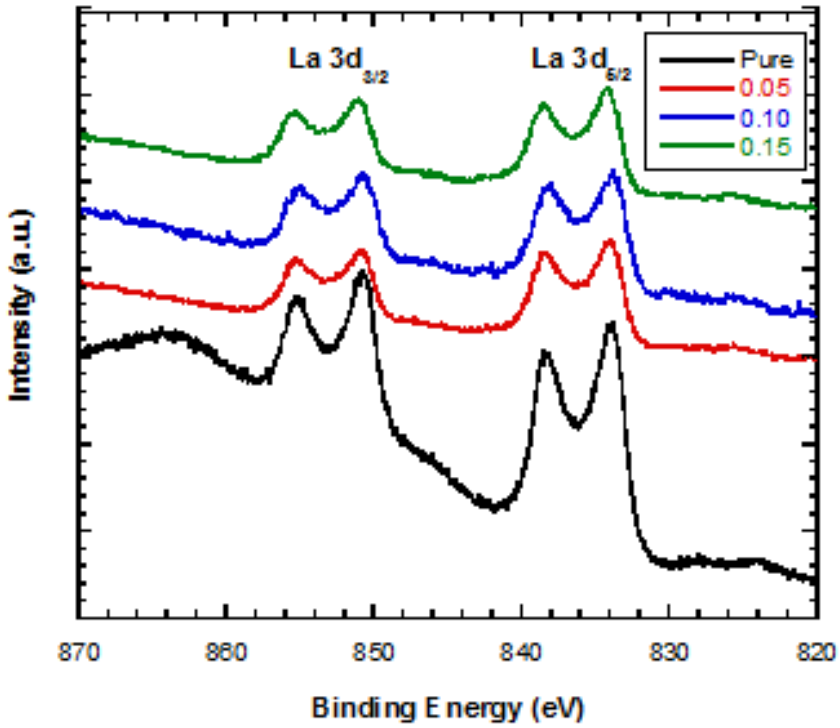

Figure 4. 10. XPS La 3d spectra of various Al-doped LLTAlO thin films.

Figure 4.10 shows XPS Ti 2p spectra of the thin films. 464 eV and 458 eV bonding energies Ti $2p_{1/2}$ and Ti $2p_{3/2}$ spin orbit separation distinction 6 eV corresponds to oxidation state of Ti^{+4} (Šalkus et al., 2011).

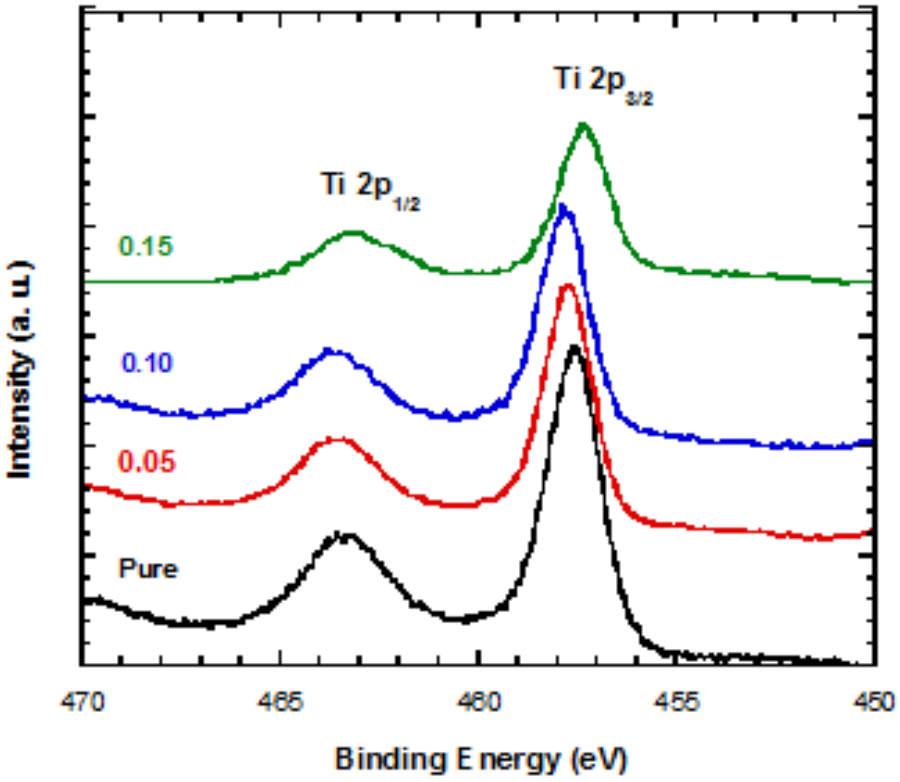

Figure 4. 11. XPS Ti 2p spectra of various Al-doped LLTAlO thin films.

4.3.4. Electrical Analyses

For ionic conductivity measurement, Al contact regions were occurred on pure and Al-doped LLTO thin films by using thermal evaporation system (Figure 4.12 (b)). As can be shown in Figure 4.12 (b) there are contact regions, which have different radius. By using this technique, effect of surface area on ionic conductivity could be investigated. Hoiki IM3590 impedance analyzer measures specific resistivity and the probe station as can be seen in Figure 4.13.

The obtained resistivity dates which have frequency range is between 0.1 Hz-200 kHz, were plotted with real and imaginer parts. Ionic conductivity is measured by the point which is imaginer part is equal to zero, from take over the real resistivity value.

$$\frac{\text{contact region}}{\text{film thickness}} \times R = \rho \qquad (4.1)$$

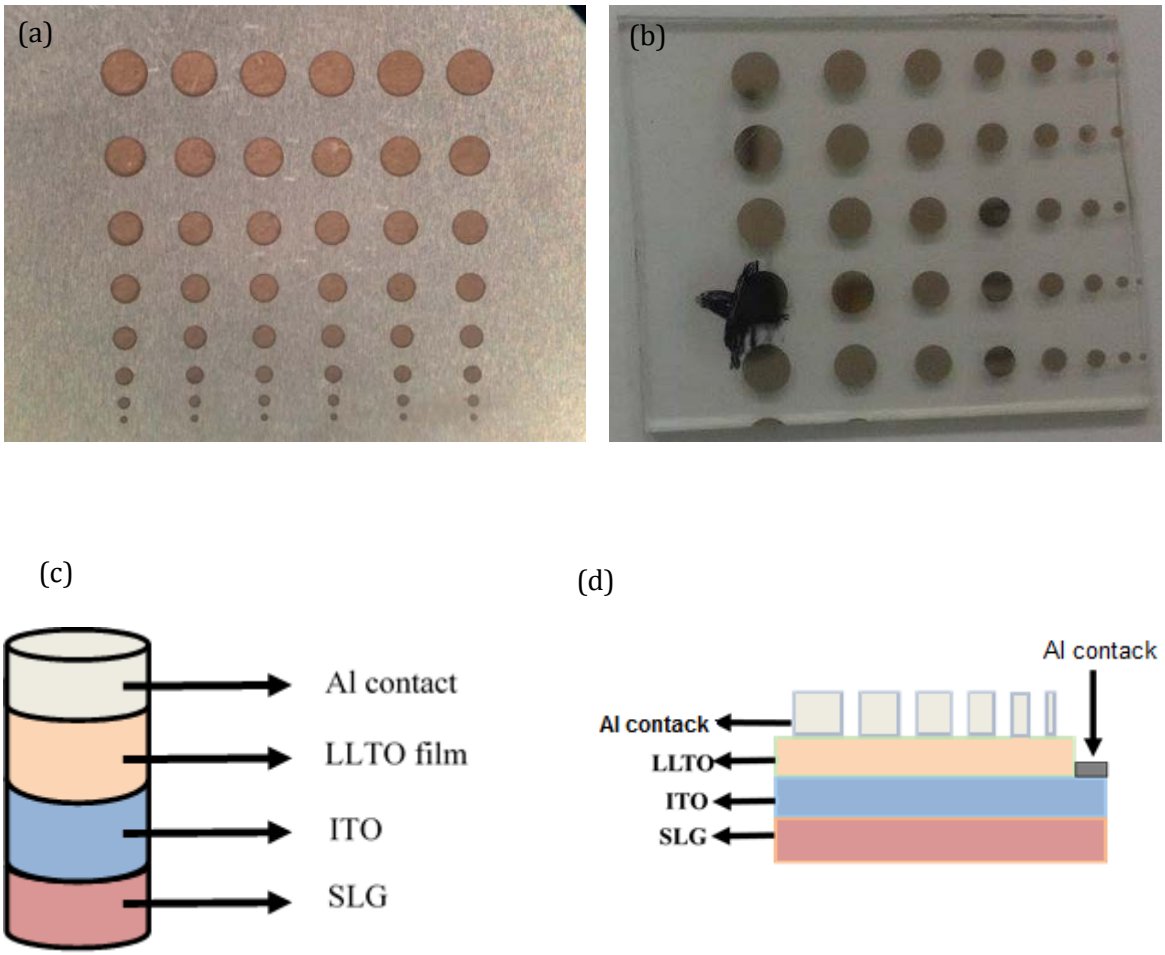

Figure 4. 12. (a) Mask for Al contact region (b) Optic microscopy picture of Al capacitance (c) Schematic picture of Al contact region (d) Cross-sectional picture of Al capacitance.

Figure 4. 13. Prop station for ionic conductivity measurement.

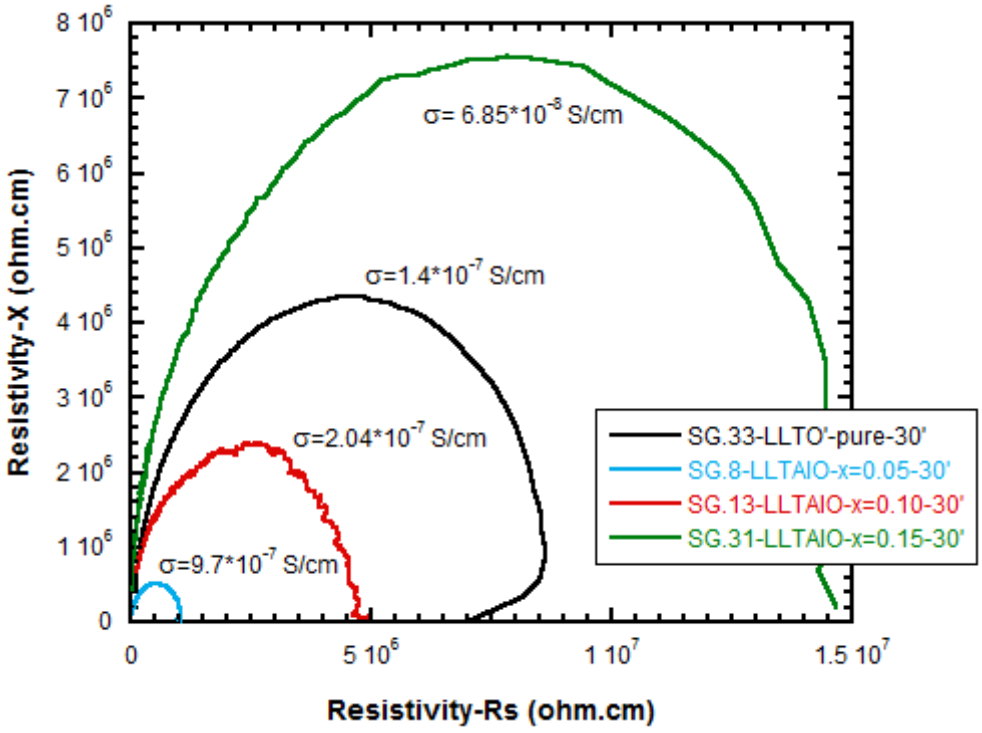

Figure 4. 14. Complex impedance spectra of pure and Al-doped samples.

Figure 4.14 shows that ionic conductivity of the pure and Al-doped LLTAlO thin films, which have the same deposition period so all the films, have approximately the same film thickness. While x=0.15 Al-doped films lower ionic conductivity, x=0.05 and x=0.10 Al-doped films have higher values. The maximum level of ionic conductivity was measured

by x=0.05 Al-doped thin film as $9.6x10^{-7}$ S/cm. It shows that Al-doping amount is increasing the ionic conductivity but so much doping effects negatively.

In LLTO 0.606 Å radius Ti^{+4} is replaced with 0.535 Å radius Al^{+3} doping causes that the decreasing of distance between the ions and increasing of bonding force. While the distance between Ti and O is decreasing, the bonding force increases, the bonding force between Li and O increases as well (He & Yoo, 2003).

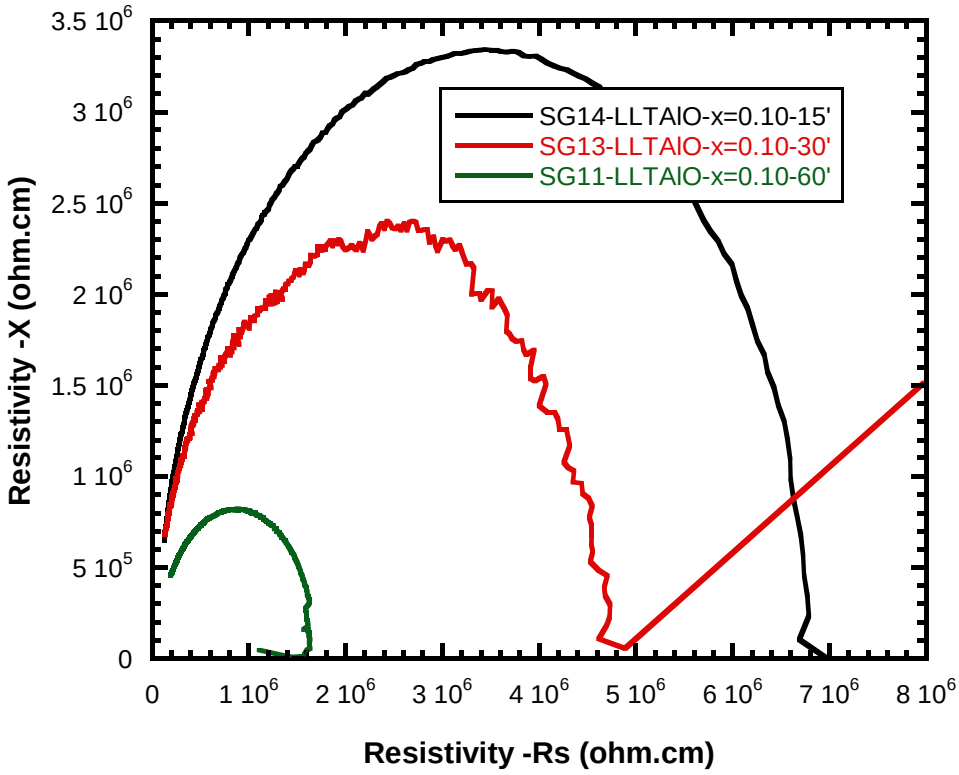

Figure 4. 15. Dependence of complex impedance spectra on various thickness of x=0.10 Al-doped LLTAlO thin film.

As can be seen in Figure 4.15 while the deposition period of the films increases the film thickness rises so the ionic conductivity increases as well.

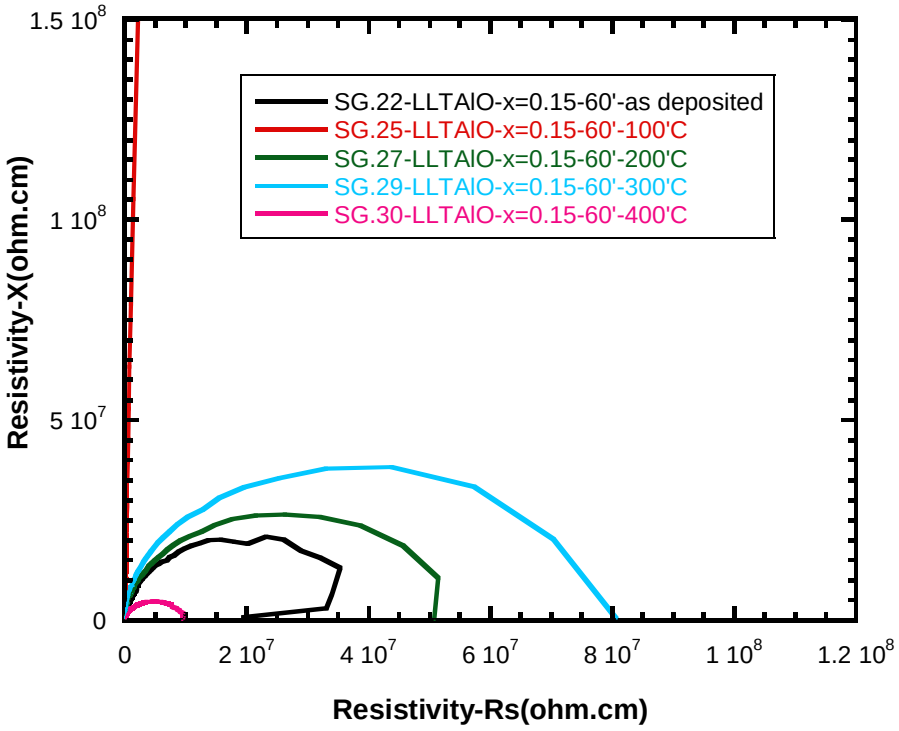

Figure 4. 16. Dependence of complex impedance spectra on various annealing temperature of x=0.15 Al-doped LLTAlO thin film.

As can be seen clearly from the Figure 4.16, when annealing temperature increases the ionic conductivity rises. Because the grain boundaries decreases by the increasing of the temperature. This result corresponds with the literature directly (Xiong et al., 2011).

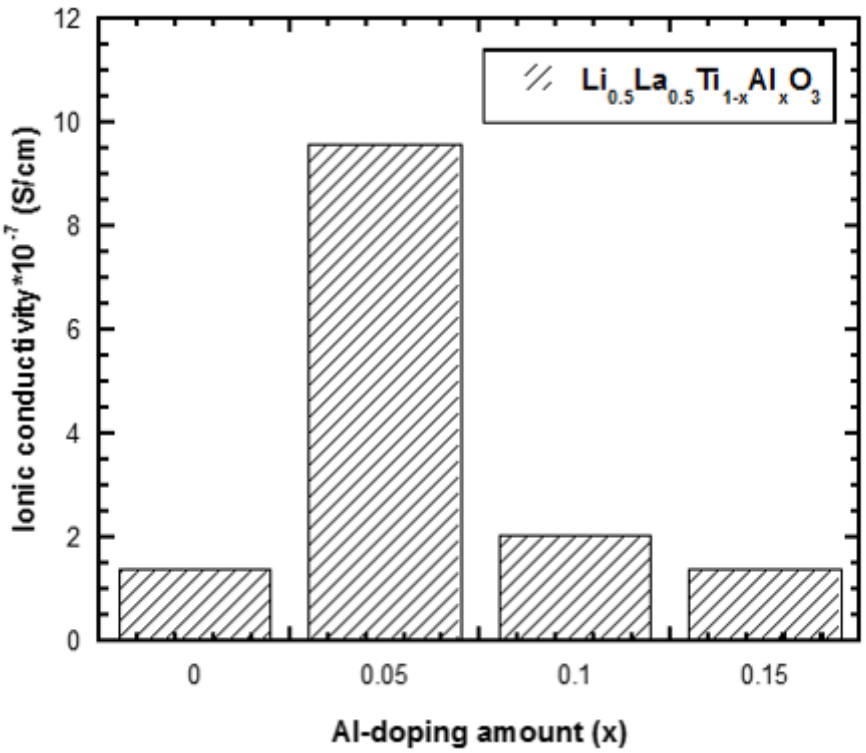

Figure 4. 17. Ionic conductivity versus Al-doping amount (x)

Al doping amount effects the ionic conductivity of the LLTO thin films. But a threshold value was determined at amount of x=0.05. If the doping ratio increases more than x=0.05, the ionic conductivity decreases. For this reason for the next studies between pure and x=0.05 Al doping, x=0.01, 0.02, 0.03, 0.04 amounts will be investigated.

(a) (b)

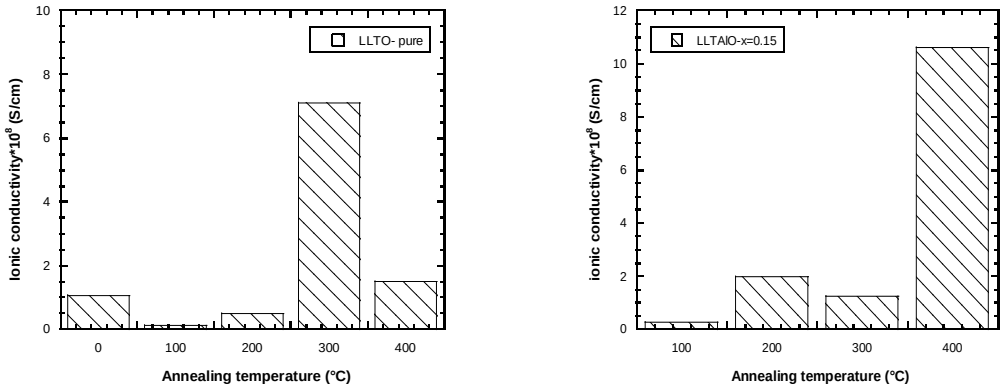

Figure 4. 18. (a) Ionic conductivity versus annealing temperature of LLTO-pure (b) Ionic conductivity versus annealing temperature of LLTAlO x=0.15.

As can be seen clearly in Figure 4.18 (a), annealing temperature is highly effective on ionic conductivities of the films. The annealed films at 300 ^{0}C have higher ionic conductivity than the other annealed LLTO-pure thin films. In Figure 4.18 (b) the highest ionic conductivity temperature is 400 ^{o}C of the LLTAlO x=0.15 thin films.

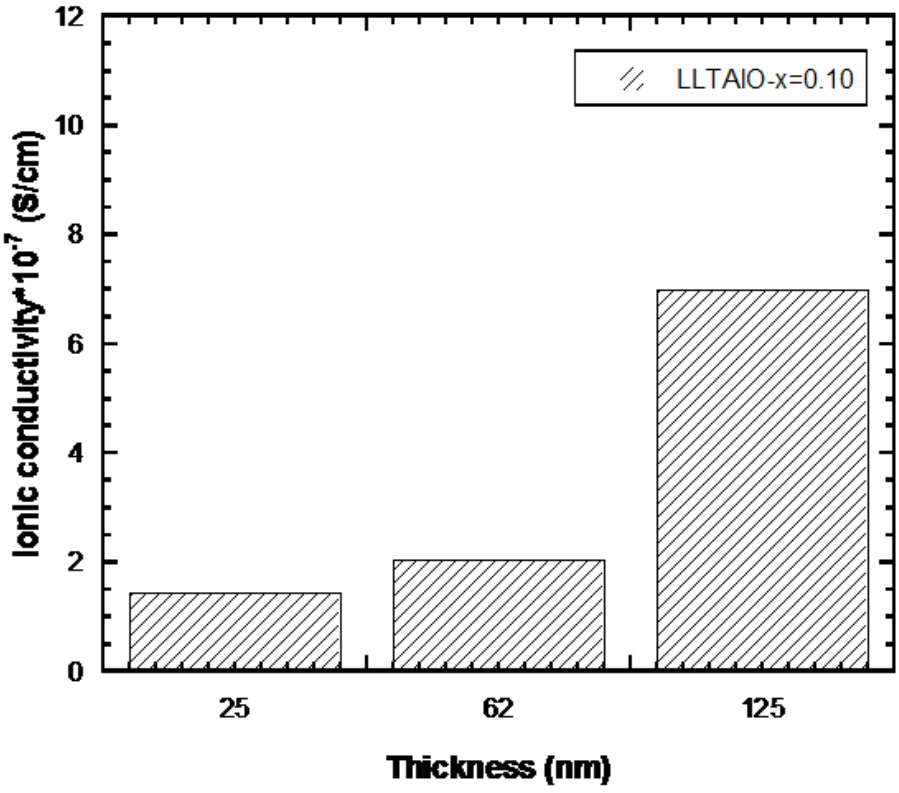

Figure 4. 19. Ionic conductivity versus thickness.

In Figure 4.19 can be seen that the ionic conductivity value depends on the thin film thickness as well. When the film thickness reaches to 125 nm the ionic conductivity value becomes maximum level.

CHAPTER 5

CONCLUSION

Pure and Al-doped LLTO targets were fabricated successfully and as structurally XRD analyses, as chemically Raman spectroscopy analyzes are completed.

It is observed that Al doping increases the crystallinity of LLTO targets.

Thin films of the targets were grown by high vacuum RF magnetron sputtering technique. Optical structural and electrical analyses are examined.

From the crystallographic results it was understood that all deposited films are amorphous, consistent with literature.

Al-doping on LLTO thin films increase ionic conductivity. But as can be understand from the results the obtained ionic conductivity values reaches the maximum level at x=0.05 amount of Al-doping. For this reason to observe higher ionic conductivity results the doping amount of x range 0.01 to 0.04 value should have consider as the range from x=0.01, x=0.02, x=0.03 to x=0.04 value. For these analyses initially the new Al-doped targets should be prepared and the new films should be growth by using the new appropriate targets.

In additionally deposition parameters can be change to convert the structure of the thin films. For example alternatively not only Ar gas can be flown through the vacuum chamber, but also oxygen gas can be flown through the chamber as reactive gas.

Furthermore, to obtain more homogeneous thin films the substrate holder can be rotate in the vacuum chamber when the plasma is occurred. At the same time there can be a new mechanism to control substrate temperature more sensitively.

Likewise, x=0.05 Al-doped thin films which have the best ionic conductivity x=0.10 Al-doped thin films and will be annealed at 100 ^{o}C, 200 ^{o}C, 300 ^{o}C and 400 ^{o}C. After than all the analyses will be repeated and compared with the other results.

Moreover Al-contact regions were generated on LLTO thin films. To observe more reliable resistivity value of the LLTO and LLTALO thin films, which are around the Al-contact regions, can be etched by any kind of etching system or material.

At last but not least ITO coated SLG substrate which was used for the ionic conductivity measurement can be replaced by another metallic substrate such as

molybdenum coated SLG. The influence of annealing temperature on LLTO thin film may be decreasing while the effect of ITO can be taken away.

REFERENCES

Abhilash, K. P., Selvin, P. C., Nalini, B., Nithyadharseni, P., & Pillai, B. C. (2013). Investigations on pure and Ag doped lithium lanthanum titanate (LLTO) nanocrystalline ceramic electrolytes for rechargeable lithium-ion batteries. Ceramics International, 39(2), 947-952. doi:10.1016/j.ceramint.2012.07.011

Aguesse, F., Roddatis, V., Roqueta, J., García, P., Pergolesi, D., Santiso, J., & Kilner, J. A. (2015). Microstructure and ionic conductivity of LLTO thin films: Influence of different substrates and excess lithium in the target. Solid State Ionics, 272, 1-8. doi:10.1016/j.ssi.2014.12.005

Ahn, J.-K., & Yoon, S.-G. (2004). Characteristics of perovskite (Li0.5La0.5)TiO3 solid electrolyte thin films grown by pulsed laser deposition for rechargeable lithium microbattery. Electrochimica Acta, 50(2-3), 371-374. doi:10.1016/j.electacta.2004.02.065

Antoniassi, B., González, A., Fernandes, S., & Graeff, C. F. d. O. (2011). Microstructural and electrochemical study of La 0.5 Li 0.5 TiO 3. Materials Chemistry and Physics, 127(1), 51-55.

Bates, J., Dudney, N., Neudecker, B., Ueda, A., & Evans, C. (2000). Thin-film lithium and lithium-ion batteries. Solid State Ionics, 135(1), 33-45.

Battery-University. (2016). Types of Lithium-ion. Retrieved from http://batteryuniversity.com/learn/article/types_of_lithium_ion

Brohead, j., A.D. Butherus (1972). 3791867. U. Patent.

Cambridge-University. (2016). Primary Batteries. Retrieved from http://www.doitpoms.ac.uk/tlplib/batteries/primary.php

Cao, C., Li, Z.-B., Wang, X.-L., Zhao, X.-B., & Han, W.-Q. (2014). Recent Advances in Inorganic Solid Electrolytes for Lithium Batteries. Frontiers in Energy Research, 2. doi:10.3389/fenrg.2014.00025

Chagnes, A. (2015). Lithium Battery Technologies: Electrolytes. Lithium Process Chemistry: Resources, Extraction, Batteries, and Recycling, 167.

Chen, R., Liang, W., Zhang, H., Wu, F., & Li, L. (2012). Preparation and performance of novel LLTO thin film electrolytes for thin film lithium batteries. Chinese Science Bulletin, 57(32), 4199-4204. doi:10.1007/s11434-012-5292-y

Chung, S.-Y., Bloking, J. T., & Chiang, Y.-M. (2002). Electronically conductive phospho-olivines as lithium storage electrodes. Nature materials, 1(2), 123-128.

Daniel, C. (2008). Materials and processing for lithium-ion batteries. Jom, 60(9), 43-48.

Di Salvo, F., Schwall, R., Geballe, T., Gamble, F., & Osiecki, J. (1971). Superconductivity in layered compounds with variable interlayer spacings. Physical Review Letters, 27(6), 310.

Dudney, N., & Neudecker, B. (1999). Solid state thin-film lithium battery systems. Current Opinion in Solid State and Materials Science, 4(5), 479-482.

Esterly, D. M. (2002). Manufacturing of Poly (vinylidene fluoride) and Evaluation of its Mechanical Properties.

He, L., & Yoo, H. (2003). Effects of B-site ion (M) substitution on the ionic conductivity of (Li 3x La 2/3− x) 1+ y/2 (M y Ti 1− y) O 3 (M= Al, Cr). Electrochimica Acta, 48(10), 1357-1366.

Hoffart, F. (2008). Proper care extends Li-ion battery life. Power Electronics Technology, 34(4), 24.

IJESD, A. (2000). Costs of lithium-ion batteries for vehicles.

Inaguma, Y., Liquan, C., Itoh, M., Nakamura, T., Uchida, T., Ikuta, H., & Wakihara, M. (1993). High ionic conductivity in lithium lanthanum titanate. Solid State Communications, 86(10), 689-693.

Inaguma, Y., & Nakashima, M. (2013). A rechargeable lithium–air battery using a lithium ion-conducting lanthanum lithium titanate ceramics as an electrolyte separator. Journal of Power Sources, 228, 250-255. doi:10.1016/j.jpowsour.2012.11.098

Kanehori, K., Matsumoto, K., Miyauchi, K., & Kudo, T. (1983). Thin film solid electrolyte and its application to secondary lithium cell. Solid State Ionics, 9, 1445-1448.

Kelly, I., Owen, J., & Steele, B. (1985). Poly (ethylene oxide) electrolytes for operation at near room temperature. Journal of Power Sources, 14(1-3), 13-21.

Kharton, V. V. (2009). Solid state electrochemistry I: fundamentals, materials and their applications: John Wiley & Sons.

Kirino, F., Ito, Y., Miyauchi, K., & Kudo, T. (1986). ELECTROCHEMICAL-BEHAVIOR OF AMORPHOUS THIN-FILMS OF SPUTTERED V2O5-WO3 MIXED CONDUCTORS. Nippon Kagaku Kaishi(3), 445-450.

Li, C.-L., Zhang, B., & Fu, Z.-W. (2006). Physical and electrochemical characterization of amorphous lithium lanthanum titanate solid electrolyte thin-film fabricated by e-beam evaporation. Thin Solid Films, 515(4), 1886-1892.

Linden, D. (1995). Handbook of batteries. Paper presented at the Fuel and Energy Abstracts.

Minami, T., Tatsumisago, M., Wakihara, M., Iwakura, C., Kohjiya, S., & Tanaka, I. (2006). Solid state ionics for batteries: Springer Science & Business Media.

Mizushima, K., Jones, P., Wiseman, P., & Goodenough, J. (1980). LixCoO2 (0< x<-1): A new cathode material for batteries of high energy density. Materials Research Bulletin, 15(6), 783-789.

Monroe, C., & Newman, J. (2005). The impact of elastic deformation on deposition kinetics at lithium/polymer interfaces. Journal of the Electrochemical Society, 152(2), A396-A404.

Murphy, D., & Christian, P. (1979). Solid state electrodes for high energy batteries. Science, 205(4407), 651-656.

Nagaura, T., & Tozawa, K. (1990). Lithium ion rechargeable battery. Prog. Batteries Solar Cells, 9, 209.

Nong, J., Xu, H., Yu, Z., Zhu, G., & Yu, A. (2015). Properties and preparation of Li–La–Ti–Zr–O thin film electrolyte. Materials Letters, 154, 167-169.

Ohtsuka, H., & Yamaki, J.-i. (1989). Preparation and electrical conductivity of Li2O-V2O5-SiO2 thin films. Japanese journal of applied physics, 28(11R), 2264.

Rao, B., Francis, R., & Christopher, H. (1977). Lithium-aluminum electrode. Journal of the Electrochemical Society, 124(10), 1490-1492.

Ritchie, A., & Bagshaw, N. (1996). Military Applications of Reserve Batteries [and Discussion]. Philosophical Transactions of the Royal Society of London A: Mathematical, Physical and Engineering Sciences, 354(1712), 1643-1652.

Šalkus, T., Kazakevičius, E., Kežionis, A., Orliukas, A., Badot, J., & Bohnke, O. (2011). Determination of the non-Arrhenius behaviour of the bulk conductivity of fast ionic conductors LLTO at high temperature. Solid State Ionics, 188(1), 69-72.

Sanjuán, M. L., Laguna, M. A., Várez, A., & Sanz, J. (2004). Effect of quenching on structure and antiferroelectric instability of La(2−x)/3LixTiO3 compounds: a Raman study. Journal of the European Ceramic Society, 24(6), 1135-1139. doi:10.1016/s0955-2219(03)00581-8

Sloop, S. E., Pugh, J. K., Wang, S., Kerr, J., & Kinoshita, K. (2001). Chemical Reactivity of PF 5 and LiPF6 in Ethylene Carbonate/Dimethyl Carbonate Solutions. Electrochemical and Solid-State Letters, 4(4), A42-A44.

Steele, B., & Van Gool, W. (1973). Fast ion transport in solids. edited by W. Van Gool, North Holland, Amsterdam, 103.

Thackeray, M., David, W., Bruce, P., & Goodenough, J. (1983). Lithium insertion into manganese spinels. Materials Research Bulletin, 18(4), 461-472.

Whittingham, M. S. (1976). Electrical energy storage and intercalation chemistry. Science, 192(4244), 1126-1127.

Xiong, Y., Tao, H., Zhao, J., Cheng, H., & Zhao, X. (2011). Effects of annealing temperature on structure and opt-electric properties of ion-conducting LLTO thin films prepared by RF magnetron sputtering. Journal of Alloys and Compounds, 509(5), 1910-1914.

Zheng, Z., Fang, H., Yang, F., Liu, Z. K., & Wang, Y. (2014). Amorphous LiLaTiO3 as Solid Electrolyte Material. Journal of the Electrochemical Society, 161(4), A473-A479. doi:10.1149/2.006404jes

Zheng, Z., & Wang, Y. (2012). 3D structure of electrode with inorganic solid electrolyte. Journal of the Electrochemical Society, 159(8), A1278-A1282.